

# Application of Shape Memory and Self-Healable Polymers/Composites in the Biomedical Field: A Review

Tejaswini Tadge,<sup>#</sup> Sonali Garje,<sup>#</sup> Varun Saxena, and Ashok M. Raichur\*



Cite This: *ACS Omega* 2023, 8, 32294–32310



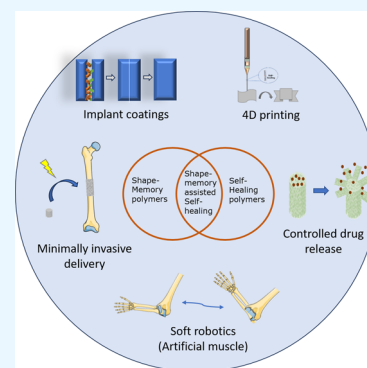
Read Online

ACCESS |

Metrics & More

Article Recommendations

**ABSTRACT:** Shape memory-assisted self-healing polymers have drawn attention over the past few years owing to their interdisciplinary and wide range of applications. Self-healing and shape memory are two approaches used to improve the applicability of polymers in the biomedical field. Combining both these approaches in a polymer composite opens new possibilities for its use in biomedical applications, such as the “close then heal” concept, which uses the shape memory capabilities of polymers to bring injured sections together to promote autonomous healing. This review focuses on using shape memory-assisted self-healing approaches along with their respective affecting factors for biomedical applications such as tissue engineering, drug delivery, biomaterial-inks, and 4D printed scaffolds, soft actuators, wearable electronics, etc. In addition, quantification of self-healing and shape memory efficiency is also discussed. The challenges and prospects of these polymers for biomedical applications have been summarized.



## 1. INTRODUCTION

Multifarious stimuli-responsive systems are found in nature in both plants and animals. Being inspired by nature, researchers have developed stimuli-responsive smart materials for a wide range of applications. Smart materials have the ability to change some of their properties in response to an external stimulus.<sup>1,2</sup> Shape memory polymers (SMPs) are an exciting category of smart materials that can recover their shape in a predetermined manner in response to certain stimuli such as pH,<sup>3,4</sup> heat,<sup>5,6</sup> light,<sup>7,8</sup> electric fields,<sup>9,10</sup> and magnetic fields.<sup>11,12</sup> First, SMPs were used as heat-shrinkable tubing and commercialized as cross-linked polyethylene.<sup>13</sup> SMPs have been utilized for different applications in the aerospace, textile, and biomedical sectors. In particular, it has attracted much interest in the biomedical community due to its capacity to facilitate minimally invasive surgery, offer skeletal support, apply stabilizing forces, and elute therapeutic molecules,<sup>2</sup> and its applications have been reviewed in recent years. For instance, Oladapo et al. investigated the application of 4D-printed artificial intelligent material (AIM) in bioengineering. Owing to the shape-morphing ability of the SMPs, they can be used for 4D printing of flexible AIM required for mimicking flexible parts of the human body. Uyan and Celiktas reviewed the utilization of natural SMPs and composites such as poly(lactic acid), lignin derivatives, vanillin, etc. Biobased SMPs overcome the environmental concerns caused by fossil-based SMPs due to their biodegradability and mimic the actuation ability of natural tissues. Moreover, investigators have also reviewed the biomedical application of SMPs and 4D printing in general medicine, nanomedicine, cancer therapy,

dentistry, orthopedics, etc. However, most of these studies have solely focused on the utility of SMPs and composites, which do not guarantee 100% recovery of material desired in the case of self-tightening sutures and staples, self-fitting bone scaffolds, and controlled-release drug delivery systems. Furthermore, with the advent of self-healing systems, it is now possible to achieve complete recovery of the structure. The self-healing ability enables the system to heal and recover from physical damage by featuring physical or chemical bonding between the cracked surfaces.<sup>14</sup> To initiate this bonding, the damaged surfaces should be placed in contact. The shape memory property assists this process by bringing the surfaces in spatial proximity.<sup>15</sup> Combining shape memory and self-healing properties in a composite resolves the individual lags of the polymeric materials (by hastening the process of wound and crack closure and improving the longevity of the implantable polymeric materials) for the aforementioned biomedical applications.

This review is precisely focused on combining shape memory and self-healing properties to be utilized for biomedical applications. We outline the primary mechanism involved in self-healing and shape memory polymers. Furthermore, the biomaterial considerations for the design of

Received: June 26, 2023

Accepted: August 22, 2023

Published: September 1, 2023

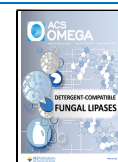


**Table 1. External Stimuli and Shape Memory Mechanism for SMPs**

external stimuli	shape memory mechanism	references
Temperature	Heating the polymer above transition temperature allows the molecular chains to move more freely, lowers its energy barrier, and increases the polymers' entropy. This helps in the deformation of the polymer matrix into a temporary shape that can be fixed by cooling and applying external forces. After exposure to a suitable external stimulus, it returns to its original shape by releasing internal stress and energy.	22
Light	Infrared light can be used to heat polymers having a thermally induced shape memory effect. By adding conductive fillers such as carbon black, carbon nanotubes, and conductive ceramics to such devices, heat transfer can be improved. Another approach utilizes chromophores onto SMPs, contributing to shape fixation in the presence of one wavelength, e.g., UV light, via photoreversible cross-linking. The shape-memory is then achieved by differing the incident light's wavelength or energy.	23 24
Magnetic field	Incorporating magnetic nanoparticles such as iron(III) oxide and neodymium–iron-boron (NdFeB) causes inductive heating of thermoresponsive SMPs in the presence of alternating magnetic fields.	25
pH	Breaking and forming the specific bonds at various pH enables shape change and recovery due to the change in the polymer's isoelectric point.	26
Water	Moisture diffuses into the temporary fixed polymeric matrix when submerged in water, acting as a plasticizer. In addition, the newly formed hydrogen bond between the polymeric chain and water molecules competes with the pre-existing inter and intramolecular hydrogen bonds. Swelling and competitive hydrogen bonding decreases the storage modulus and $T_g$ , leading to permanent shape recovery.	27

self-healing and SMP-based systems and the methods for their quantification are discussed. Additionally, we decipher the limitations and challenges associated with shape memory and self-healing polymers, along with their future prospects.

## 2. SHAPE MEMORY AND SELF-HEALING APPROACH

The self-healing ability of polymers is contingent on their cross-linking and polymeric orientations, which also underscores their shape-memory properties. These approaches are discussed below:

**2.1. Shape Memory Approaches.** SMPs can change their shape temporarily, which can be recovered in the presence of external stimuli, as discussed in the introduction section. The shape memory effect in the polymers is attributed to the presence of permanent and reversible phases in the polymeric matrix. A permanent phase of the polymeric matrix typically uses covalent cross-links to maintain the original shape, and the reversible phase consists of physical cross-links, responsible for the stimuli-responsive recovery through the transitions such as melting or glass transition.<sup>16</sup> Table 1 summarizes the mechanism for the shape-memory effect of polymers using various external stimuli. Structural and intrinsic properties of polymers such as high shape fixity and recovery, intrinsically higher modulus, greater chemical and thermal stability, adequate recovery rate, and longer life cycle are essential to be considered to produce the high-performance SMPs.<sup>17</sup> The shape memory effect of SMPs can be affected by the composition, cross-linker type, cross-linker density, and process parameters used during its fabrications.<sup>18,19</sup> For example, Behera et al. used an ionic-liquid cross-linker to improve the shape fixity of polyurethane, which was compromised with a nonionic cross-linker. This is because the ionic-liquid cross-linker in the hard segment makes it incompatible with the soft segment and improves phase separation, which is a critical requirement for thermoplastic SMPs.<sup>19</sup> Further, the process parameters such as the heating/cooling rate and scaffold dimensions affect the shape memory effect of SMPs. Pisani et al. demonstrated the enhanced shape memory effect and faster shape recovery rate of SMP nanofibers (SMPNs) compared to SMP films; this behavior is likely due to the faster fiber heating/cooling rate due to their large surface area compared to films obtained by solvent casting. Besides, many other fiber parameters, such as fiber diameter, porosity, orientation, and morphology, can influence shape memory effect and must thus be optimized.<sup>20</sup>

Furthermore, it is also critical to examine the typical requirements of a biomaterial, such as biocompatibility, biodegradability, mechanical properties, and sterilizability in the SMPs, for its plausible application in the biomedical sector.<sup>21</sup>

**2.2. Self-Healing Approaches.** Self-healing is the ability of a material to recover from physical damage through physical or chemical interactions (Figure 1). Self-healing materials are

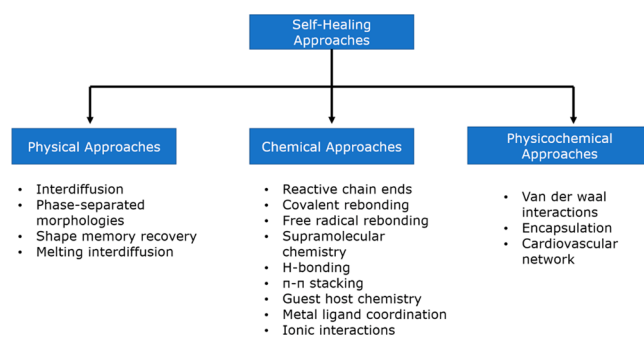


**Figure 1.** Various interactions involved in self-healing of a polymeric matrix.

categorized into two categories, namely extrinsic<sup>28</sup> and intrinsic,<sup>29</sup> based on the mechanism of healing. In an extrinsic system, a healing agent is integrated into the polymeric network, which is released after physical damage and aids in network repair. Two approaches are used in extrinsic repair, i.e., capsular and vascular. Capsule-based self-healing materials utilize capsules, which contain healing agents. As the capsules rupture, the healing agents are released, and their respective reactions in the damaged location help the materials' repair. The local healing agent is depleted after release, resulting in just one instance of local healing.<sup>30</sup> The healing agent is incorporated into the interconnected capillary or hollow channels in the vascular self-healing materials. After damage, healing agents are delivered through capillary networks that heal the damaged fractions. Unlike capsular-based systems, vascular self-healing materials enable several local healing processes by refilling the network through the healing agent present in the undamaged network.<sup>31</sup>

In contrast to extrinsic self-healing systems, intrinsic self-healing materials heal without any external healing agent; the interaction between the reactive ends of the polymer repairs

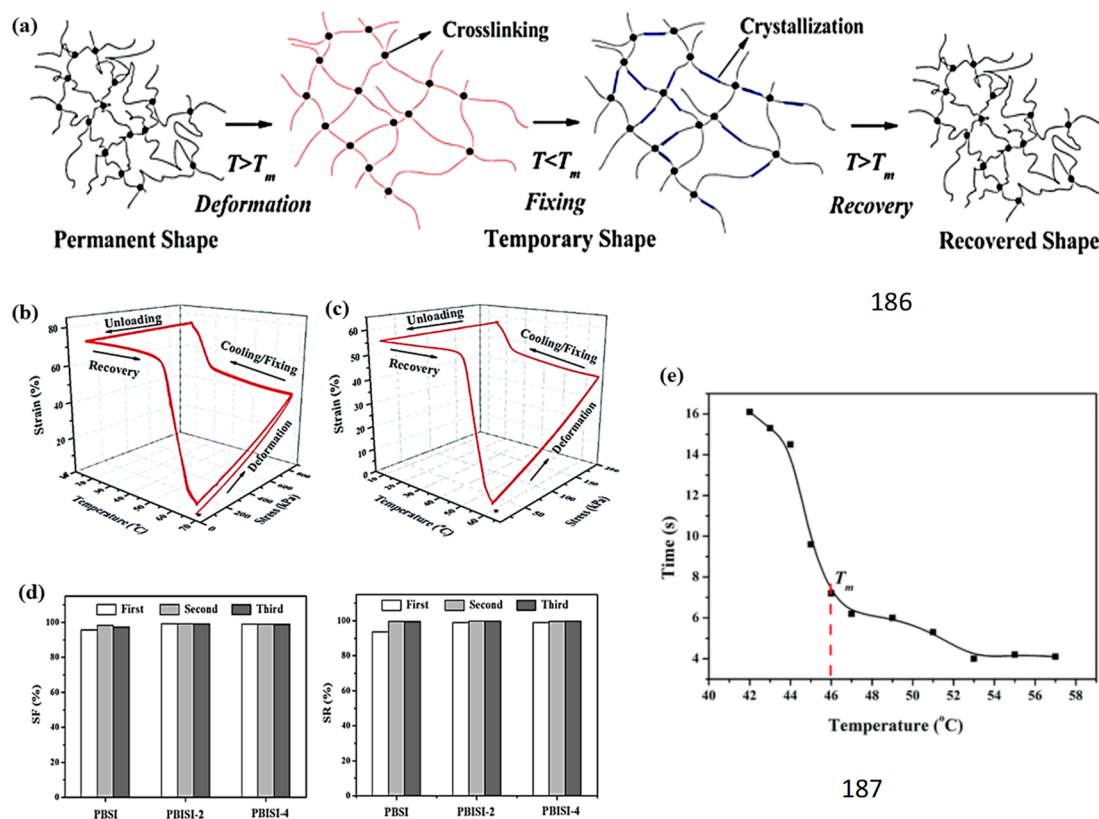


**Figure 2.** (a) Schematic representation of PBISI-based SMP's mechanism during shape recovery. 3D diagrams of stress-controlled programming cycles for the (b) PBISI SMP and (c) PBISI-2 SMP. An asterisk denotes the initial point of the cycling process. (d) Graph showing percent shape fixity and shape recovery of PBISI-based SMPs. (e) Shape recovery time of PBISI-2 SMP scaffold with temperature (adapted from ref 45).

the network intrinsically. Moreover, intrinsic self-healing is based on noncovalent or dynamic covalent interactions.<sup>32</sup> Noncovalent interactions include host–guest interaction,<sup>33</sup> hydrogen bonding,<sup>34</sup> ligand–metal bonding,<sup>35</sup> and  $\pi$ – $\pi$  stacking,<sup>36</sup> while covalent approaches use dynamic urea bonds,<sup>37</sup> Diels–Alder (DA) reaction,<sup>38</sup> trans-esterification,<sup>39</sup> etc. Covalent approaches such as DA cross-linking have shown advantages not only in the development of SMPs, but it has also enabled simultaneous development of self-healable systems. For instance, Mondal et al. developed recyclable and self-healable SMPs using PMMA. A macro-RAFT agent based on a 3-arm star PCL as a starter was used to synthesize a self-healing SMP with soft polycaprolactone (PCL) and hard poly(furfuryl methacrylate) (PFMA) domains. The hard domains of the precursor polymer were cross-linked via a thermoreversible DA “click” reaction with 1,1'-(methylene-4,4,1-phenylene)bismaleimide to produce a DA network. After deformation at higher temperatures and subsequent cooling, the soft PCL segments let the polymer adapt to a new temporary shape, whereas the rigid, chemically DA cross-linked PFMA domains push the polymer to return to its original shape after reheating. In addition, the polymer is endowed with thermoreversible furan–maleimide DA links, which enables self-healing and recyclable materials that can be used in various applications such as biomedicine, electronics, aerospace, etc.<sup>40</sup> Similarly, Raut et al. utilized DA chemistry to cross-link a fluorescence active elastomer. The adaptable covalent linkages in the thermoreversible DA chemistry of elastomer enabled it to display chemosensing, reprocessability, recyclability, and self-healing properties.<sup>41</sup> Moreover, multiresponsive self-healing systems can be developed utilizing different cross-

linking interactions. For example, Banarjee et al, developed dual responsive self-healable hydrogels by introducing both covalent (DA) and noncovalent cross-linking (ionic interactions).<sup>42</sup>

### 3. QUANTIFICATION OF SHAPE MEMORY EFFICIENCY

Shape memory efficiency (SME) is defined and quantified using shape fixity (SF) and shape recovery (SR) that characterize the material's programmability and recoverability, respectively.<sup>43–45</sup> The thermoviscoelastic theory model is used to describe the thermodynamic behavior of SMPs. For example, if a molecular chain of a polymer resembles a little spring, the springs entangle when mixed because of their smaller diameter and considerable length. It has higher entropy since the springs in SMPs are positioned arbitrarily at ambient temperature. The polymer becomes more mobile at higher temperatures, making it thermoviscoelastic. An external stimulus may stretch and align the springs, reducing the polymer's entropy. Furthermore, if the temperature is lowered without varying the external stimulation, the polymer loses thermoviscoelasticity, which weakens the molecular motion and hinders the springs from returning to their original shape. This process converts the stress stored in the molecular chains into elastic potential energy. As the temperature increases again, the spring releases this stored elastic potential energy, reacquiring the thermoviscoelasticity.<sup>46</sup> This explains the role of molecular processes like structural and stress relaxation in defining the shape memory effect and its time dependence.<sup>47</sup>

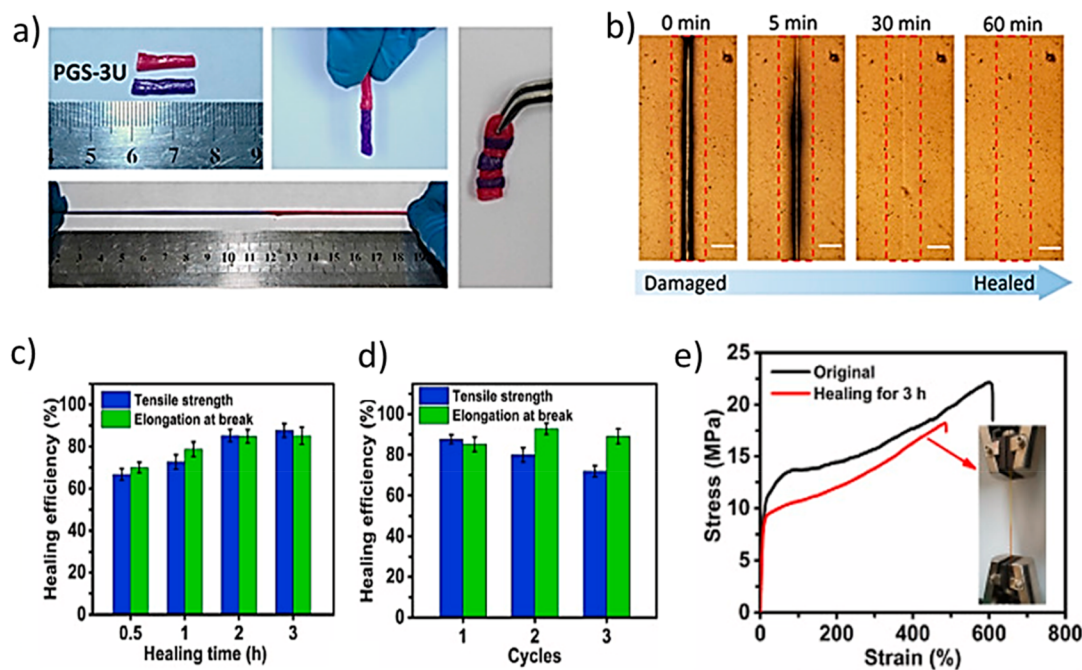


**Figure 3.** (a) Dyed red and blue PGS-U films enable visualization of interfaces that close when pressed for 5 min at 55 °C. (b) Optical images of superficially damaged and healed PGS-U samples at 55 °C with time. Scale bar: 200  $\mu\text{m}$  (adapted from ref 55). (c) Healing efficiency of EMNa/EMA-30 at different cycle times. (d) Healing efficiency of EMNa/EMA-30 at different cycle times. (e) Stress–strain curves for both original and healed EMNa/EMA-30 (adapted from ref 58).

Taking account of the viscoelastic and entropic contributions of synthetic polymers to SME, a cyclic thermomechanical analysis should be performed.<sup>48,49</sup> From a practical perspective, it is crucial to consider the stress–strain–temperature–time relationship, which is the most fundamental way to assess SMP, and the straightforward constitutive equation that illustrates the relationship.<sup>50</sup> For this purpose, a dynamic mechanical analyzer is used that generates the thermomechanical shape memory cycles. The experiments are performed by heating the samples above their respective melting temperature ( $T_m$ ) and then deforming them by increasing the force from a preload to an intended strain ( $\epsilon_m$ ), followed by cooling the sample to  $T_{\text{fix}}$  below the  $T_m$  while retaining the force. To ensure the shape fixation, the forces on the samples are released, resulting in programmed/fixed strain  $\epsilon_f$  at a constant temperature  $T_{\text{fix}}$  below  $T_m$ . Following it, the material is heated at a constant rate, without the application of any external force, and allowed to recover its strain  $\epsilon_r$  freely. The following equations can be used to measure the shape recovery ratio ( $R_r$ ), shape fixity ratio ( $R_f$ ), and recovery rate ( $v_r$ ).

$$R_r = \frac{\epsilon_m - \epsilon_r}{\epsilon_m} \quad (1)$$

$$R_f = \frac{\epsilon_f}{\epsilon_m} \quad (2)$$

$$v_r = \frac{R_r}{\Delta T_r} \quad (3)$$

where  $\Delta T_r$  is the temperature interval over which shape recovery occurs.<sup>51</sup>

It is also necessary to determine the recovery time. For this purpose, the time taken by a sample with a temporary shape to return to its permanent shape under the given stimulus is measured.<sup>52–54</sup> For example, Kang et al. fabricated a thermally

induced biobased poly(butanediol/isosorbide/sebacate/itaconate) (PBISI) SMP. It exhibited elastomeric behavior above its  $T_m$  and was deformed into a temporary shape. The temporary shape fixation occurred by cooling SMP below its  $T_m$ , followed by its recovery on reheating (Figure 2a). Further, cyclic thermomechanical tests were performed to quantify the shape memory behavior of PBISI-based SMPs (Figure 2b,c). The SF and SR values increased with the increase in the cycle times and isosorbide concentration in the scaffold (Figure 2d). Among all, PBISI-SMP 2 rapidly recovered in almost 16 s at around 42 °C (Figure 2e).<sup>45</sup>

#### 4. QUANTIFICATION OF SELF-HEALING EFFICIENCY

One of the essential aspects of self-healing materials is measuring their healing efficacy. The self-healing efficiency (HE) can be determined both qualitatively and quantitatively. For qualitative analysis, the self-healing scaffolds are first fabricated by adding dyes such as crystal violet, Nile red, and fluorescein isothiocyanate (FITC) to the polymer solution. The stained scaffolds are then cut into two symmetric parts using a razor blade, and the wounding edges of differently stained parts are placed together. The scaffolds are then allowed to heal, and the healing process is visualized using a camera (Figure 3a).<sup>55,56</sup> However, visual inspection using a camera is not an efficient method to check the self-healing ability of the material. Another way to analyze self-healing is by making a scratch on the surface of the scaffold and then heating the sample at a particular healing temperature. This technique observes the scratch damage healing process under an optical microscope (Figure 3b).<sup>57,58</sup> The interface between the two surfaces can be observed to inspect its self-healing ability. Yaobin et al. prepared the self-healable supramolecular bio elastomers using poly(glycerol sebacate)-graft-ureidopyrimidinone (PGS-UPy). The polymer films of PGS-3UPy were

colored (red and blue) to differentiate between the interfaces, and the samples were easily pressed at 55 °C for five min to weld those pieces. The self-healing process was then recorded by using the camera. Optical images of superficially damaged and thermally healed PGS-UPy samples (55 °C) for different time points were captured (Figure 3a,b).<sup>55</sup> Moreover, to quantify the self-healing efficiency, the pristine and healed scaffolds are subjected to a tensile test, and the HE is calculated by the following equations:

$$\text{HE}_{\text{stress}} = \frac{\sigma_{\text{healed}}}{\sigma_{\text{original}}} \times 100\% \quad (4)$$

$$\text{HE}_{\text{strain}} = \frac{\varepsilon_{\text{healed}}}{\varepsilon_{\text{original}}} \times 100\% \quad (5)$$

where  $\sigma_{\text{original}}$  and  $\varepsilon_{\text{original}}$  are the initial tensile strength and elongation at break, respectively, and  $\sigma_{\text{healed}}$  and  $\varepsilon_{\text{healed}}$  are the tensile strength and elongation at break of the healed specimens, respectively.<sup>58–61</sup> Yan et al. prepared the self-healable blend of poly(ethylene-co-methacrylic acid) sodium ionomer (EMNa) and poly(ethylene-co-methyl acrylate) (EMA). The self-healing efficiency of the specimens was quantified by using static uniaxial tensile measurements. As the healing time increases, the healed samples' tensile properties match the initial samples, showing improved HE with healing time (Figure 3c). However, it decreases with repeated healing cycles and still possesses tensile strength and elongation at a break of 15.9 MPa and 543.1%, respectively, after 3 h of healing (Figure 3d,e).<sup>58</sup>

## 5. APPLICATIONS

SMPs and self-healing polymers (SHPs), because of their reversible shape change and interaction-specific stimuli responsiveness, have been utilized for a broad spectrum of applications. A few of them are discussed below.

**5.1. Tissue Engineering.** Tissue engineering aims at developing organ and tissue substitutes to restore and improve the functions of damaged or injured tissues.<sup>62</sup> Herein, a carrier scaffold locally delivers the cells and growth factors at the injury site.<sup>63</sup> However, a surgical procedure is required to transplant a scaffold that often causes unwanted effects, such as postoperative pain and delayed recovery. Researchers are exploring minimally invasive surgical approaches to minimize such trauma associated with the surgical implantation of scaffolds. One such method is to use a deployable shape memory-based self-healable scaffold that can be implanted via minimally invasive surgery.

Researchers have examined different approaches to obtain the SME and HE for biomedical applications. In this section, we have discussed a few such examples along with their respective efficacy. For instance, Shaabani et al. developed an aniline trimer (AT) incorporated shape memory-based self-healable polyurethane scaffold (PU-AT scaffold) capable of regulating the differentiation of human adipose-derived mesenchymal stem cells to osteogenic lineage. The scaffold exhibited excellent shape memory with shape fixity and recovery ratios of >98% and >97%, respectively. It could also heal intrinsically near the body temperature with an efficiency of around 95%. Furthermore, it promoted osteoblast attachment and proliferation due to its inherent bioactivity and electroconductivity, thereby potentiating its application as a cancellous bone scaffold in the area of minimally invasive

surgery.<sup>64</sup> Second, to address the demands of practical surgery, Yang et al. prepared polydopamine particles (PDAPs) reinforced poly(vinyl alcohol) (PVA) hydrogels stabilized by hydrogen bonding. The hydrogels endowed shape memory due to the crystallization of the PVA chains by a repeated freeze–thawing process and its melting on exposure to NIR light. Together with shape memory, it also presented the ability to self-heal because of the photothermal nature of PDAP that raised the localized temperature of the damaged area and encouraged PVA chains to move and reform the hydrogen bond. As this hydrogel mimics the actuation and healing ability of native tissues, it can potentially be used in fabricating artificial cartilage and skin tissues.<sup>65</sup> In another work by Fu et al., double network hydrogels were developed, where dibenzaldehyde-terminated telechelic poly(ethylene glycol) and *N*-carboxyethyl chitosan (CEC) formed the first network through imine bonds, and the polyacrylamide served as the second network. The reversibility of imine bonds in pH provided self-healing and pH-responsive shape memory and the ability of CEC to form a complex with metal ions endowed metal ligand-responsive shape memory to the hydrogels. Due to such properties, it could also be utilized in multiple applications, such as a deployable scaffold in tissue engineering, an actuator in soft robotics, and in smart wearable electronics.<sup>66</sup>

Fabricating wound dressings and sutures is another area where shape memory-assisted self-healing polymers are explored. The traditional surgical sutures speed up the wound-healing process. However, knotting creates peculiar challenges for medical professionals. Particularly, when the knotting force is too high, necrosis occurs in the surrounding tissue, increasing the risk of subsequent infection in the injured area. The self-healable SMP-based sutures avoid the risk of infections associated with knotting of sutures by pulling the wound edges closer, which then close and self-heal. In this regard, Sun et al. synthesized SMP based on the ring-opening polymerization of 2-methyl-2-benzoyloxycarbonyl propylene carbonate (MBC), which was found to be a potential candidate for wound dressing. The elastomer demonstrated self-healing characteristics at 25 °C due to the noncovalent interactions between the polymer chain.<sup>67</sup> The self-healing behavior of the elastomer can further be tuned to a desired efficiency by varying the temperature, as increasing the temperature can drive polymer motion and encourage the reformation of hydrogen and hydrophobic bonds.<sup>67–69</sup>

Similarly, Li et al. fabricated zwitterionic SMP-based wound dressing to address the issue of adhesion-based conglutination and to promote faster wound healing via shape memory-assisted self-healing.<sup>70</sup> Hence, researchers have been able to design polymers responsive to physiological conditions to obtain SME and HE for potential biomedical applications. Such materials are promising, in terms of their stability, responsiveness, and compatibility, and can be used in tissue engineering after clinical trials.

**5.2. Drug Delivery.** The SMP-based drug delivery systems have gained tremendous attention because of (1) their potential to facilitate the minimally invasive delivery of the depot and (2) their ability to recover the shape upon exposure to appropriate stimulation, thereby controlling the drug release.<sup>71</sup> The self-healing feature of a hydrogel enables it to be injected locally in the sol form, where it recovers rapidly into a gel-like structure and prevents the washout of drug-loaded polymers from the injected site.<sup>72</sup> When both

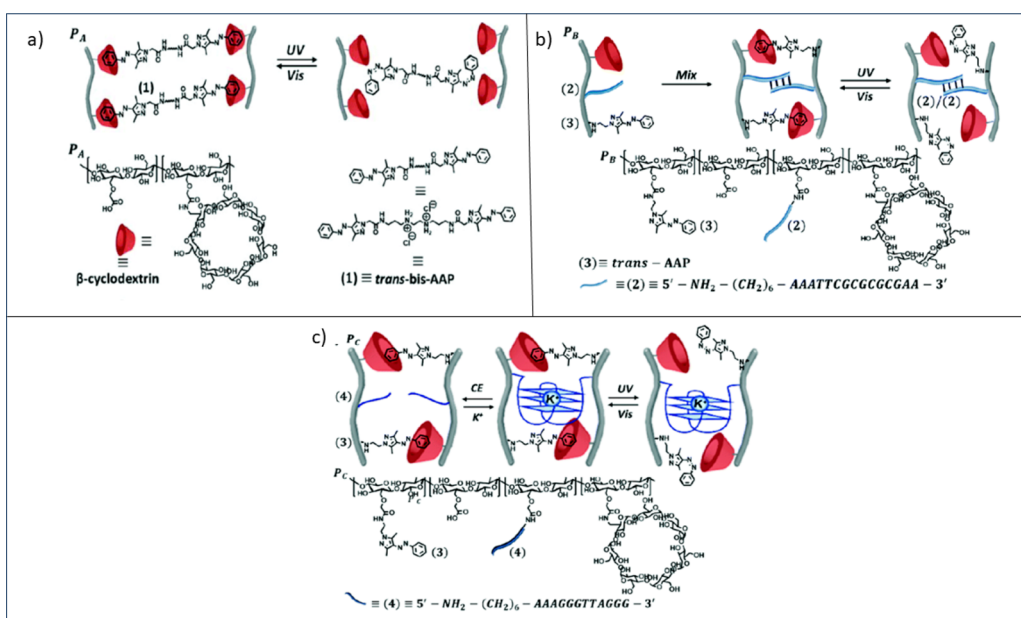


**Figure 4.** Schematic showing switchable control of the stiffness characteristics of the functionalized CMC polymer scaffold. (a) Light-induced trans/cis isomerization of bis-AAP for cross-linking and partial separation of the polymer chains. (b) A hybrid CMC hydrogel that has been cooperatively cross-linked by  $\beta$ -CD/trans-AAP and nucleic acid. (c) Hydrogel matrix with dual-triggered (UV and CE) stiffness characteristics made up of  $\beta$ -CD/trans-AAP and  $K^+$  ion stabilized G-quadruplexes (adapted from ref 73).

properties are combined, the shape memory recovers the hydrogel structure to some extent, retrieving it completely by self-healing. This helps release the drug via shape change upon stimulation and ceasing the release completely via shape memory-assisted self-healing of the matrix. Gilad et al. developed arylazopyrazole (AAP) based hydrogels that exhibited light-induced stiffness modulation (shape memory). For this purpose, (i) they functionalized carboxymethylcellulose (CMC) with  $\beta$ -cyclodextrin ( $\beta$ -CD)/bis-trans-AAP (Figure 4a) and  $\beta$ -CD/trans-AAP/nucleic acid tethers (Figure 4b), forming a stiffer hydrogel network. Upon exposure of the UV light, the trans to cis isomerization of bis-AAP resulted in the dissociation of bis-cis-AAP/ $\beta$ -CD interactions, partially reducing the stiffness of the hydrogel (Figure 4a,b). (ii) In the second case,  $K^+$  ion stabilized G-quadruplexes and  $\beta$ -CD/trans-AAP complexes worked together to stabilize the hydrogel, endowing dual responses, photochemical (UV/vis) and chemical (in the presence of crown ether), which led to a programmable switch for modulating the stiffness and achieving control over the drug release (Figure 4c). The authors indicated that the release of the drug was different under different incubations. For instance, approximately 34 nmol of DOX was released from 2 mg of the low-stiffness hydrogel after being exposed to UV light for 10 min, and approximately 25 nmol of DOX was released from the same amount of hydrogel after being exposed to CE for 30 min.<sup>73</sup> This indicates that using the SHPs, the release of the drug can be controlled based on stimuli.

In the same way, Liu et al. also developed two types of controlled-release DNA-based polyacrylamide hydrogels. In one case, the hydrogel matrix was stabilized by  $K^+$  ion-stabilized G-quadruplex units and glucosamine-boronate ester bridges. The hydrogel transitioned from a stiffer matrix system to a quasi-liquid matrix and *vice versa* in the presence of the crown ether and  $K^+$  ions, respectively. In another type of hydrogel matrix, a trans-azobenzene-stabilized duplex nucleic

acid and glucosamine-boronate ester bridges worked together to cross-link the hydrogel and provided light-responsive stiffness modulation to the system. In both cases, the permanent cross-linking of the hydrogel by the glucosamine-boronate ester bridges provided the memory code and the switchable moieties responsible for the hydrogels' chemical/light-responsive self-healing.<sup>74</sup>

Another research study by Wang et al. led to the development of thermoresponsive, controlled release matrices. The polyacrylamide chains were cross-linked with bis-acrylamide-nucleic acid duplexes/boronate ester-glucosamine-nucleic acid duplexes and incorporated with gold nanoparticles/nanorods (AuNPs or AuNRs). The plasmonic heating of the AuNP/AuNRs loaded hydrogels led to the dehybridization of the DNA duplexes that reduced their stiffness and promoted drug release. After the light source was turned off, the shape memory provided by the permanent cross-linking and self-healing due to nucleic acid hybridization regained the stiffer state and controlled the drug release.<sup>75</sup> Xu et al. prepared a similar type of thermoresponsive hydrogel based on gelatin UPy. The hydrogel showed thermally responsive shape fixation and recovery owing to the formation and disruption of the UPy dimer on cooling and heating, respectively. Additionally, the  $Fe^{3+}$  ion-induced gelatin cross-linking endowed self-healing ability to the hydrogel and controlled the release of 5-fluorouracil.<sup>76</sup>

Furthermore, enzyme-guided switchable control over hydrogel stiffness offers new ways to create biocatalytically driven shape-memory and self-healing matrices. The biocatalytic control of pH, in response to the respective substrates, leads to the reversible switch over the stiffness of the hydrogel. These qualities were explored for substrate-triggered controlled drug release. Wang et al. integrated glucose oxidase (GOx) into a DNA-based hydrogel, where glucose-guided pH changes led to insulin release. Glucose-triggered regulation of the hydrogel's stiffness and the glucose dose-controlled insulin

release offer different modes for the released insulin to independently regulate blood glucose levels.<sup>77</sup> Another pH-responsive hydrogel was fabricated by Qiao et al. using poly(diacetone acrylamide-co-acrylamide-co-acrylic acid) (PDAAc), diacylhydrazine-terminated PEG (PEGDH), and alginate. The fabricated hydrogel exhibited doxorubicin release of almost 100% in acidic pH due to the dissociation of the acylhydrazone bond between the carbonyl groups of doxorubicin and acylhydrazine groups of PEGDH. Additionally, it possessed self-healing ability because of the reformation of hydrogen bonds between the carboxyl group of acrylic acid, protonated alginate, and amide groups and the acylhydrazone cross-linking between PEGDH/PDAAc copolymer. Moreover, it was able to present shape fixation and recovery due to ionic cross-linking in the  $\text{FeCl}_3$  solution and its disruption in the EDTA solution, respectively. Even though this hydrogel's self-healing and shape memory properties have no contribution to drug release, it broadens the scope of the pH-responsive hydrogel in biomedicine.<sup>78</sup>

In wound healing, replenishing the hydrogel for additional drug loading disturbs the wound-hydrogel interface and the healing process. Self-healable hydrogels show a tendency to attach over the other hydrogel surface and transfer the drug from the bulk of one hydrogel to another via diffusion. This avoids the need to replace the hydrogel patch with a replacement from the wound surface. Nayak et al. fabricated a DNA-carbon dot-poly(vinylpyrrolidone) (DNA-CD-PVP) hydrogel with self-healing and shape memory properties. Hemin was loaded into a DNA-CD-PVP hybrid hydrogel as a model drug, and the hydrogel proved to be capable of sustained hemin delivery. The hemin-loaded part of the hydrogel was self-healed with the hemin-unloaded hydrogel, and hemin diffusion occurred from the loaded to unloaded part of the hydrogel during the self-healing process. The hydrogel's remarkable biocompatibility, stimuli responsiveness, and effective antimicrobial activity through visible-light-induced ROS generation potentiates its use in wound healing applications.<sup>79</sup> Various studies on controlled drug release via light-, chemical-, and enzyme-guided modulation over shape changes and stiffness are still under research. Clinical validation of such systems and translational scientific innovation in this area will change the future of drug delivery. Moreover, injectability, targeting, and controlled drug delivery can be combined simultaneously to increase patient compliance and make therapy more beneficial.

**5.3. Self-Healable Biomaterial-Inks and 4D Printed Shape Morphing Scaffolds.** A new biofabrication technique called four-dimensional (4D) bioprinting integrates time as a fourth dimension with three-dimensional (3D) bioprinting, enabling the bioprinted constructs to change their shape or function over time in response to an external stimulus.<sup>80</sup> 4D bioprinting fabricates complex scaffolds for biomedical applications such as tissue engineering<sup>81–83</sup> and drug delivery.<sup>80</sup> The 3D-printed hydrogel constructs may possess the risk of delamination under large deformation due to the lack of interlayer adhesiveness. The shape memory and self-healing properties of 4D bioprinted hydrogels are highly desired for fostering interlayer adhesion and enhancing the scaffold's structural integrity. Further, the self-healing property enables the biomaterial ink to automatically reconstruct through a dynamic reversible interaction after being extruded through the nozzle. It improves the mechanical properties of the scaffold postprinting.<sup>84</sup> Kuang et al. combined shape-

memory and self-healing attributes to synthesize novel bioink of highly stretchable semi-interpenetrating polymer network (semi-IPN) via UV-light assisted direct-ink-write printing. The bioink was prepared from the urethane diacrylate and linear polycaprolactone (PCL), which acted as a healant for self-healing behavior and as the switching phase for shape memory. The hydrogen bond between urethane and the diffusion/entanglement of PCL chains are two structural characteristics that may be responsible for the shape-memory and self-healing ability of semi-IPN elastomer.<sup>85</sup>

Diba et al. developed photoreactive gelatin nanoparticles (GNPs) based colloidal ink that could self-heal upon extrusion and print a construct with shape memory. The GNPs were modified with methacryloyl moieties to impart photoreactive functionality. The gel showed covalent and noncovalent interactions due to pendant methacryloyl groups and the inherent moieties ( $\text{NH}_3^+$  and  $\text{COO}^-$ ) in the gelatin structure, respectively. The noncovalent interactions allowed the gel to self-heal upon experiencing the damage associated with the extrusion-based shear forces. On the other hand, upon printing, the UV-induced covalent cross-linking enabled the scaffold to memorize the shape, withstand larger mechanical stresses, and provide control over the degradation, swelling, and bio/molecule release (Figure 5).<sup>86</sup>

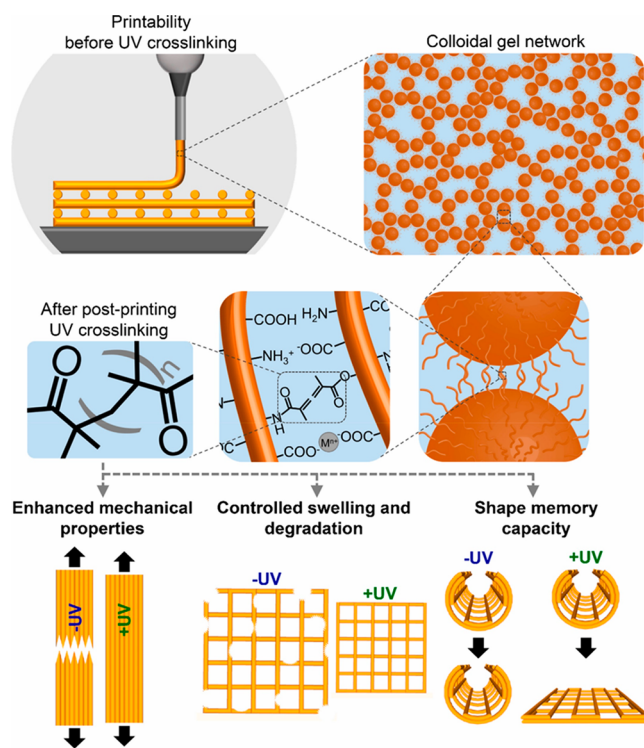


**Figure 5.** Diagrammatic representation of the gelatin-based colloidal inks used in extrusion-based 3D printing, their architecture at various length scales, and significant characteristics of printed scaffold facilitated by UV cross-linking (adapted from ref 86).

Similarly, taking advantage of the reversible interactions between the gelatin and PU NPs, Wu and Hsu fabricated a self-healable hybrid bioink that could print a shape memory scaffold for the minimally invasive delivery.<sup>84</sup> Wang et al. also investigated the potential of a gelatin-based hydrogel in 4D printing. They prepared imine/Diels–Alder cross-linked hydrogel using amino-functionalized gelatin and polyethylene

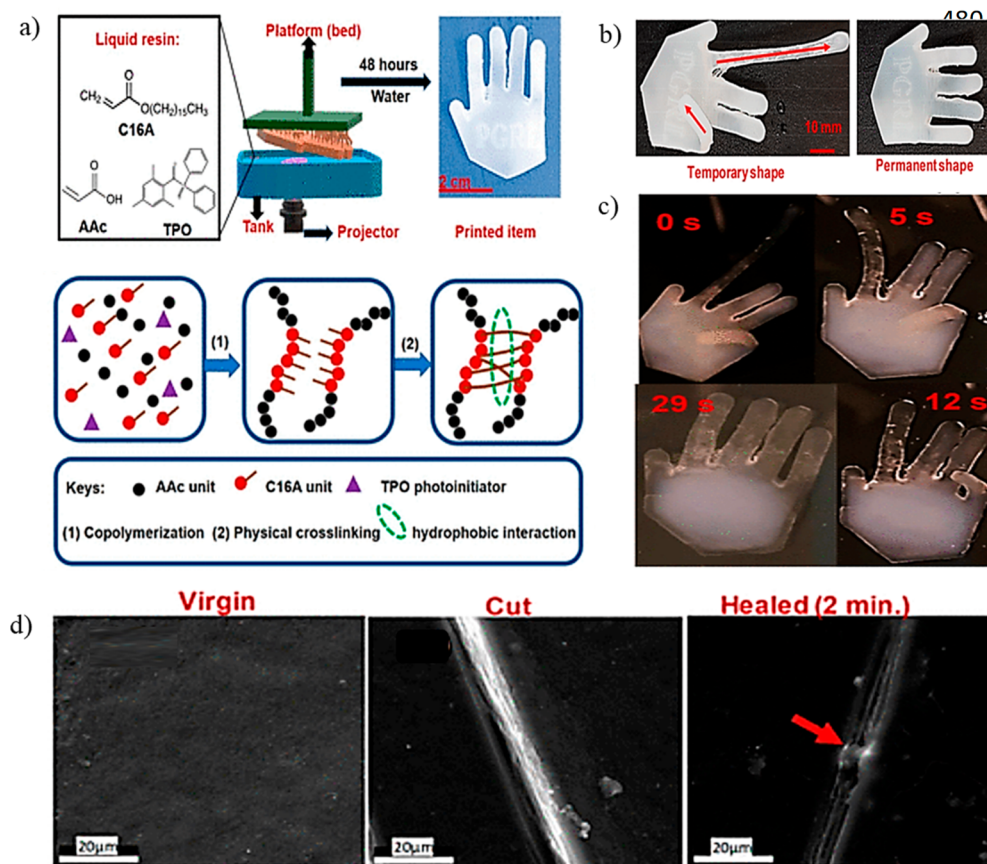


**Figure 6.** (a) Schematic depicting the synthesis of PAAC hydrogels containing C16A units via stereolithography. (b) A printed robotic hand in temporary and permanent shapes. (c) and the shape-recovery process in water at 43 °C. (d) SEM pictures demonstrating the beginning of the healing process (adapted from ref 93).

glycol (PEG) and further introduced a hyperbranched triethyl siloxane reagent (HPASi) in the network. The double crosslinking in the hydrogel network contributed to the improvement in the mechanical properties and enabled the hydrogel to self-heal. Further, the temperature-responsive behavior of HPASi imparted shape memory to the hydrogel at around 65 °C.<sup>87</sup> These studies thus provide new opportunities for the minimally invasive application of gelatin-based constructs as deployable or tissue-conforming structures that, once implanted in the body, can conform to a particular defect shape.

**5.4. Soft Actuators and Wearable Electronics.** Inspired by the adaptable, soft, and deformable bodies found in nature, soft robotics have been developed and considered safer for interactions with the human body. It can be used as a wearable sensory skin, human-assisting actuators, prosthetics, artificial organs, body-part simulators, drug delivery devices, rehabilitation, and assistance owing to the soft nature of the materials.<sup>88,89</sup> However, biocompatibility and biomimicry of soft robotics need to be considered for their application in the biomedical field.<sup>89</sup> SMPs provide compliant actuation in soft robotics, necessary for its applications in the biomedical field.<sup>90</sup> By destruction of the temporary network in SMPs, in response to the intended stimulus, automatic shape recovery takes place. This provides the actuating force required to create soft actuators. Although the softness of the material used in soft robotics offers many advantages, it is also responsible for the damage to the material in a dynamic environment. SHPs address this issue by recovering the damage through intrinsic

healing and increasing soft robotics's mechanical properties and lifetime.<sup>91</sup>

Actuation is mainly performed by muscles, a soft connective tissue capable of contracting in response to a physiological stimulus inside the host body. In biological processes, the connective tissues can self-heal, owing to the presence of fibroblast cells. Here, the self-healing ability is exceptionally crucial, as in the cases of intense stress and strain the muscles can be torn or even broken. Hence, the material must possess self-healing and actuation abilities to fabricate the natural muscle mimetic hydrogel system. To fulfill this requirement, Banerjee et al. developed an organic–inorganic nanocomposite hydrogel system based on physical and covalent cross-linking. Upon damage or injury, the hydrogel exhibited stimuli-triggered self-healing in neutral and acidic pH. It also exhibited shape memory and stimuli (salt, acid, and electric impulse) driven actuation behavior in water. Moreover, it could be fabricated into an artificial muscle, as it can restore mechanical integrity after failure and actuate whenever required.<sup>92</sup>

Recently, researchers created mechanically robust hydrogels with shape memory and self-healing properties that can be printed via stereolithography (SLA). The hydrogels were synthesized by copolymerizing hydrophobic hexadecyl acrylate (C16A) segments with hydrophilic poly(acrylic acid) (PAAC) polymeric chains (Figure 6a). The reassociation of hexadecyl side chains above its melting point and the hydrophobic interactions within the network bestowed the self-healing property to the hydrogel. Further, utilizing SLA, a robotic hand was printed that was programmed into a temporary shape at 43



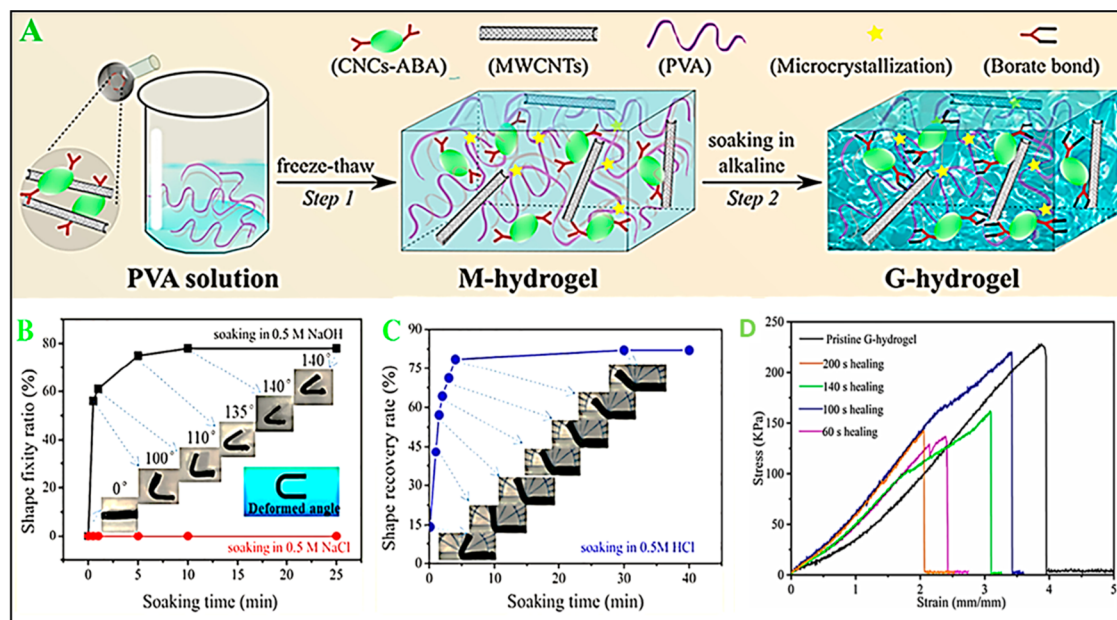


**Figure 7.** (A) Schematic presentation of fabrication of electroconductive hydrogel. (B) Shape fixity ratio ( $R_f$ ) curve of G-shape hydrogel for various times of soaking in alkaline solution. (C) The G-hydrogel shape recovery ratios ( $R_r$ ) curve an alkaline solution for various soaking times. (D) The healing efficiency of G-hydrogel curves for different healing times under NIR light (adapted from ref 98).

°C by folding one digit and stretching another, followed by shape fixation at 20 °C (Figure 6b). The hand was then submerged at 43 °C to examine the shape memory. The outcome demonstrated simultaneous recovery from folding and stretching, and the printed hand regained its original shape in less than 1 min of recovery (Figure 6c,d).<sup>93</sup> This showed the enormous potential of C16A and PAAc copolymerized hydrogels in a wide range of fields, especially where dynamic adaptation is necessary, such as soft robotics, aerospace, and biomedical applications.

Another study by Zhao et al. showed the fabrication of high-strength polymeric hydrogels that can be used to design soft actuators, because of their self-healable and shape memory properties. This was achieved by cross-linking PAA with graphene oxide and  $\text{Fe}^{3+}$  ions. The PAA cross-linking by graphene oxide helped increase the hydrogel's strength. At the same time, the ionic cross-linking between the  $\text{Fe}^{3+}$  ions and carboxyl groups of the PAA helped in modulating the strength. In the presence of  $\text{FeCl}_3/\text{HCl}$ , the free  $\text{COO}^-$  groups of PAA formed an ionic bond with the  $\text{Fe}^{3+}$  ions, forming a more rigid hydrogel. When the dual physically cross-linked hydrogel was immersed in HCl solution, the  $\text{Fe}^{3+}$  ions swapped with  $\text{H}^+$  ions, decreasing the cross-linking density and weakening the hydrogels. The strength of the hydrogels decreased from 1.8 to 0.9 MPa, and the breaking strain increased from 330 to 770% as the concentration of HCl was increased from 0.1 to 0.3 M. This reversible switch provided a shape memory effect to the hydrogel and, in turn, tuned its mechanical strength. It also showed self-healing upon the damage, as in the presence of  $\text{FeCl}_3/\text{HCl}$ , it presented a bridging effect by forming a bond with the  $\text{COO}^-$  groups of damaged PAA chains.<sup>94</sup>

Furthermore, inspired by the bending behavior of *Mimosa*, Xue et al. designed and fabricated a flexible catcher actuator. Poly(vinyl alcohol)-borax (PVA/borax) hydrogel interpenetrated with poly(1-allyl-2-thiourea-co-acrylamide) (P(ATU-co-AM)) formed a semi-interpenetrating network. At alkaline pH, the formation of borate bonds stabilized the hydrogel

backbone in a temporary shape. However, the hydrogel regained its original shape in HCl because of the reversible nature of the borate bond. Similarly, when placed in the solution of  $\text{Ca}^{2+}$  ions, the thiourea domain in the hydrogel combined with the  $\text{Ca}^{2+}$  ions led to an S-Ca-S cross-linking, holding the hydrogel in a temporary shape. Moreover, it was reversed when the  $\text{Ca}^{2+}$  cross-linked hydrogels were placed in deionized water. By this approach, a flexible actuator was constructed that caught a toy fish by shrinking in the  $\text{Ca}^{2+}$  solution and returned the toy by swelling in deionized water. Along with actuation, it also showed  $\text{Ca}^{2+}$  ions assisted self-healing, which showed its applicability in complicated designing of soft actuators and wearable electronics.<sup>95</sup>

Similarly, Lv et al. developed flexible hydrogels using natural polysaccharides such as locust bean gum (LBG) and gellan gum (Gg). LBG/Gg molten solution was mixed with borax, forming boron ester bonds with LBG. Further, when the mixture was cooled, a change from the spiral form of Gg chains to helix occurred and proceeded from single helix to double helix via hydrogen bonding. This mechanism of forming boron-ester and hydrogen bonds on subsequent heating and cooling endowed the self-healing ability to the damaged hydrogel network. Further, the protonation and deprotonation of borate ions at acidic and alkaline pH led to the disruption and reformation of the LBG network, respectively. This provided pH-responsive shape memory to the hydrogels, enhancing its potential in developing complicated actuator designs with simple triggers of actuations such as pH.<sup>96</sup> Another pH-responsive hydrogel was fabricated by Lu et al. Dopamine (DA) grafted PEG was cross-linked with the irreversible covalent bonds and reversible metal-ligand complexes. The reversibility of metal ligand coordination bonds by pH enabled the hydrogel to recover its original shape and heal intrinsically, while the covalent bonding endowed shape memorization and improved the maximum fracture stress and strain up to 65 KPa and 563%, respectively, for the hydrogels with DA:  $\text{Fe}^{3+}$  molar ratios of 1:1. Consequently, the

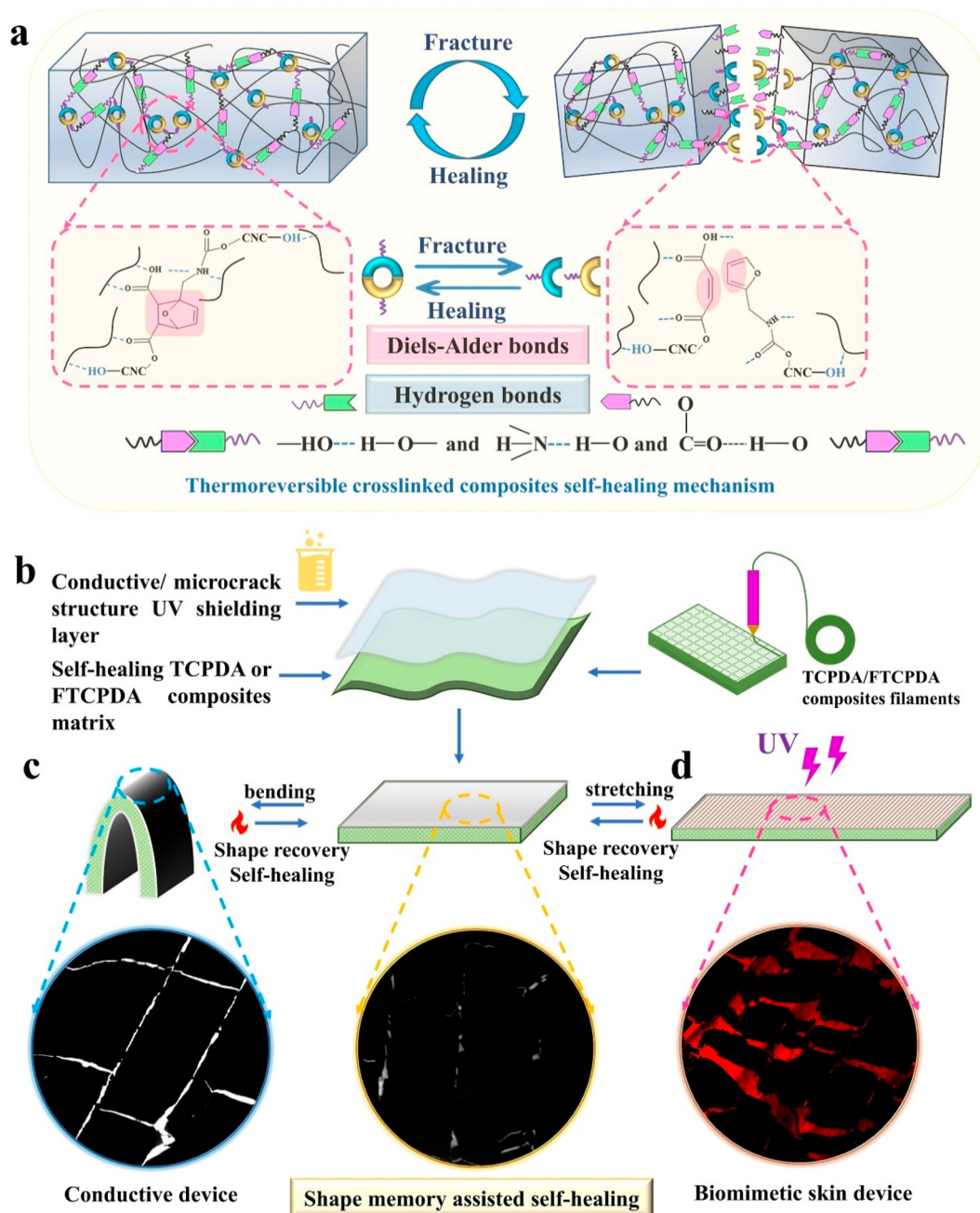


**Figure 8.** Material design: (a) the self-healable thermoreversible cross-linked polymer composites with dynamic cross-linking network design; (b) compositional schematic of the multifunctional composites; and shape memory assisted self-healing performance demonstration in the self-healing process of (c) conductive device and (d) bionic skin fluorescence device (adapted from ref 111).

simple actuation, self-healing ability, biocompatibility, and excellent mechanical properties showed the utility of this hydrogels in porosity robotics.<sup>66</sup>

Soft stretchable hydrogels have become more popular for fabricating wearable, flexible electronics due to their soothing and skin-mountable properties. However, many current hydrogel electronics are frequently prone to dryness, which causes reduced stretchability and imprecise signal extraction. Hydrogels are also expected to be significantly brighter in healing physical damage and enabling performance manipulation. Wu et al. prepared cryopolymerized polyampholyte gels with self-healing, shape memory, and antidehydration properties. Incorporating glycerol provided antidehydration properties to the hydrogel, improving the stretchability and strain-

sensing performance of the sensing electronics for long-term monitoring. Self-healing and shape memory were made possible by the dynamic properties of ionic bonding in the polyampholyte gel, which were controlled by alternate NaCl and H<sub>2</sub>O treatments. As a result, the sensing electronics could automatically repair physical damages without compromising their sensing performance. After healing, conductivity and strain-sensing performance might return to their original levels and can be adjusted temporarily owing to their shape-memory function. Cryopolymerized polyampholyte gels with qualities such as shape memory, self-healing, and antidehydration can inspire the creation of flexible, long-lasting gel-based electronics to monitor human motion.<sup>97</sup> In another work by Xiao et al., shape memory-based self-healable hydrogels were

fabricated for wearable strain sensors to increase their longevity and to provide programmable shape control. Poly(vinyl alcohol) (PVA) hydrogels incorporated with multiwalled carbon nanotubes (MWCNTs) and phenylboronic acid grafted cellulose nanocrystals (CNCs-ABA) were fabricated (Figure 7A). The pH-responsive dynamic borate bonds in the hydrogels resulted in remarkable shape recovery and fixity ratios of 82.1% and 78.2%, respectively (Figure 7B,C). However, the exceptional photothermal action of MWCNTs and reversible microcrystallization enabled 97.1% healing efficiency in just 2 min (Figure 7D). The hydrogels also achieved excellent mechanical properties due to the double cross-linking networks, and the combined effect of MWCNTs and alkali compounds increased the conductivity of the hydrogel. Additionally, the hydrogel showed excellent biocompatibility, and a quick resistance response to applied strain, making it a suitable strain sensor for monitoring human health.<sup>98</sup> Ling et al. also prepared L-cysteine-modified PVA hydrogels by creating an interpenetrating network with hydroxyethyl cellulose based on reversible covalent bonds and supramolecular hydrogen bonding. The hydrogels showed self-healing of the damaged part via disulfide and hydrogen bond reconstruction. It also showed shape memorization based on the formation of hydrogen-bond-associated microcrystals upon freeze–thawing and its disruption on reheating. Such hydrogels can be used to fabricate smart wearables.<sup>99</sup> Much research on developing wearable flexible electronics is ongoing to improve the functionality and longevity of wearable electronics. SMPs with self-healing ability have offered many advantages and opportunities to overcome the drawbacks of traditional soft robotics by enhancing their functional skills.

**5.5. Other Miscellaneous Applications.** In addition to the applications stated in the preceding sections, shape-memory polymers have been investigated for various additional uses. For example, self-healable and shape memory materials could also be used in microrobots.<sup>100</sup> Microrobots have demonstrated considerable potential for microscale activities like drug delivery, cell modification, biosensing, and micro-assembly.<sup>101</sup> Zhang et al. developed self-healable hydrogel using polyethylene glycol (PEG) and poly(10-hydroxy decanoate) (PHDA) based PU. By providing appropriate  $T_m$  and  $T_c$ , the deformation and shape fixation of the PEG/PHDA segment were observed, mainly due to the melting and crystallization phenomenon, respectively. Further, on reheating above the  $T_m$  of both PEG/PHDA segments, the PU recovered its original shape and healed intrinsically via the formation of disulfide bonds.<sup>100</sup> Based on the outcome and material properties, they mainly envisioned its application in fabricating smart microrobots.

Another potential application of SMPs' based self-healing polymeric composites includes a coating material. Magnesium metal's bioactivity, biodegradability, and biocompatibility are beneficial for developing medical implants.<sup>102</sup> Magnesium alloys, however, have a greater rate of corrosion due to their active chemical properties and low standard electrode potential. This restricts its use as an implantable material.<sup>103,104</sup> Researchers are examining to control the degradation of magnesium alloy by various approaches such as micro-alloying,<sup>105</sup> heat treatment,<sup>106</sup> surface coating,<sup>107,108</sup> and surface treatment.<sup>109</sup> Coatings can prevent the corrosion of metals by preventing or delaying the accessibility of corrosive liquids to metals. However, long-term stability of the coating is essential for adequate corrosion protection. Jiaojiao et al.

developed a double-layer coating of SMPs to solve the lacuna of the strength of anticorrosive coatings. 1,2,3-Benzotriazole, BTA (corrosion inhibitor), and ceresin wax microparticles comprise the bottom layer, and a superamphiphobic fluorinated attapulgite (fluoroATP) is the top layer. The fluoroATP layer on top could effectively block the permeation of corrosive electrolytes to the metal by providing an air cushion at a solid–liquid interface. The basal SMP-BTA layer, on the other hand, could heal the damaged area by shape memory assisted self-healing and also prevent corrosion by releasing BTA. This could control the degradation of magnesium alloy and increase its applicability as an implantable material.<sup>110</sup>

Biomimetic skin-like materials can sense the external stimulus and adapt the shape accordingly. Researchers are trying to fabricate biomimetic skin devices that mimic natural skin's mechanical and sensory performance.<sup>111</sup> The healing chemistry of the self-healing polymer and associated composites cannot take over due to the lack of adequate contact under extreme damage conditions. A shape memory-assisted self-healing approach may be able to address this issue. The shape memory effect makes it possible for the damaged surface to be nearby and for the reactive portions to reassociate across the interface. Bi et al. used thermoreversible thermoplastic PU and PCL composites to fabricate 3D printable conductive and biomimetic skin devices with good mechanical and electric healing performance. For this purpose, cellulose nanocrystalline was grafted with the furan methylamine (FA) and maleic anhydride (MAH), separately followed by cross-linking with the thermoplastic PU and PCL via reversible Diels–Alder reaction and hydrogen bonding (Figure 8). The Diels–Alder reaction chemistry played a vital role in the reversibility of the covalent bond with the temperature. As the temperature rose in the fused deposition melting printing process, the cross-linking network dissociated during its extrusion from the nozzle. However, after cooling, it cross-linked due to the reversibility of the Diels–Alder bond, thereby improving the mechanical strength of printed materials.<sup>111</sup>

Similarly, Lan et al. developed thermoresponsive hydrogel stabilized by the PAAc/diethylenetriamine (DETA) associated hydrophobic microdomains and the ionic cross-linking of DETA and PAAc. The disruption and formation of PAAc/DETA stabilized hydrophobic microdomains on heating and cooling enabled shape fixing and recovery of the hydrogel, respectively. Moreover, the reversible physical cross-links in the hydrogel bestowed intrinsic self-healing. As the properties of this hydrogel mimic the self-healing ability of skin and provide easy actuation as of muscles, it is hoped to be used in fabricating artificial skin or muscle.<sup>112</sup> This indicates that the conductivity in the polymers help reform or actuate muscles more dominantly than the nonconducting polymers.

Due to its smart functionality, shape memory, and self-healing materials can also be used in pharmaceuticals and anticounterfeiting industries. Functionally, responsive luminous gels have become promising innovative materials because luminescence, as a responsive signal, is more sensitive to external stimuli. The lanthanide-based hydrogels are more suitable for such applications than the luminous gel generated by integrating organic chromophores because of the lanthanide complex's outstanding luminescent features such as a long lifetime, a significant Stokes shift, and a line-like emission. Furthermore, lanthanide-based luminous gels exhibit tunable luminescence, stimulus responsiveness, and self-healing capa-

bilities due to dynamic lanthanide coordination. Zhou et al. combined 3,5-dinitrosalicylic acid (DNSA), catechol-grafted carboxymethyl chitosan, phenylboronic acid-grafted gelatin, and  $\text{Eu}^{3+}$  ions in aqueous solution followed by a heating–cooling procedure to fabricate the luminous lanthanide-based hydrogel. The resulting composite hydrogel responded to temperature, acid/base, salt, and redox stimuli by changing color and phase in reversible ways. This hydrogel exhibited information encryption capabilities, glucose sensing with the naked eye, shape memory performance, and improved mechanical qualities based on multiple responsiveness. Due to the dynamic bonding and combined antibacterial effects of the lanthanide complex and chitosan derivatives, it demonstrated self-healing and antibacterial activity, respectively. The fabricated hydrogel held potential in various industries, including smart wearables, sensors, anticounterfeiting, and pharmaceuticals.<sup>113</sup>

Most biopolymer hydrogels' mechanical strength and responsiveness are typically weak, severely restricting the development of intelligent hydrogels for practical applications. Double network gel, which has two or more interpenetrated polymer networks, typically has more mechanical strength and toughness in comparison to pristine materials. It also combines the multistimuli responsiveness of each polymer network. Yan et al. fabricated agar/carboxymethyl chitosan-metal ions doubled network (DN) hydrogel by incorporating carboxymethyl chitosan into an agarose gel, which is thermally reconfigurable and adsorbs the metal ions on the surface of the gel. With the degradation of the hydrogel, metal ions diffused from the composites and showed antibacterial activity. Two kinds of physical cross-links present in the hydrogels are reversible and functionally independent, so it is possible to program the hydrogel to have a variety of functions, such as pH-regulated shape memory behavior, multistage self-healing capabilities, and long-lasting antibacterial activities. Fabrication of such a coordination-driven DN gel may help develop biopolymer-based multifunctional hydrogels in nanocomponent assembly and soft electrical biosensing systems.<sup>16</sup> SMPs' based self-healing materials are currently being explored for diverse applications and have paved the way toward developing various technologies.

## 6. CHALLENGES OF SME AND SHE

As discussed earlier, SMPs are intelligent materials that can maintain their transient states and return to their starting states in response to various stimuli like solutions, light, electricity, and more. Numerous (physiological) factors, including temperature and moisture and remotely triggerable SMPs that utilize electromagnetic fields, ultrasound, etc., have been observed to cause SMEs. However, the similar dependence of SMEs restricts their application for biomedical applications to the site of action primarily. A significant obstacle for biological researchers is the limit of such polymers' responses to multiple stimuli. It is challenging to construct homogeneous SMPs because physiological conditions differ from host to host and organ to organ.

However, aside from the requirement for stimulus responsiveness, a variety of other difficulties must be considered before the development of SMPs and SHPs. These difficulties are mentioned below;

**6.1. Activation.** SMEs and SHEs are both activated through some external stimulus. It has been suggested that a variety of factors, such as body heat, ambient heat, lasers, and

more can trigger the shape-memory effect.<sup>7</sup> However, differing temperature ranges in the host body, immunogenic reactions, and a few other factors can also produce the same temperature range. This may prevent the SMPs' required activation, especially for injectable SMPs. Temperature stimuli become a restriction and barrier because the temperature ranges inside the host body are constrained to a particular range, namely, 37 °C. For example, Styrene-based thermomechanical SMPs, have a lot of potential in the biomedical field. Still, their activation and responsiveness are limited by their transition temperature range of 62 to 43 °C,<sup>114</sup> which limits their biotechnological applications. Similarly, additional activations such as lasers,<sup>115</sup> electric fields,<sup>10</sup> and magnetic fields<sup>11</sup> restrict the biomedical applications of SMPs and SHPs due to the potential injury to normal cells. Additionally, magnetic-stimuli-induced hyperthermic reactions can cause temperatures to rise to undesirable levels, which limits the possible applications of SMPs and SHPs.

**6.2. Biodegradation.** Biodegradation is a crucial concern for any biomaterial researcher. An SMP's limitations regarding water absorption, enzymatic breakdown, degraded byproducts, carcinogenicity, and immunogenicity, once injected into a host body, remain the key obstacles to its biomedical applications. For any biomaterial to be used effectively, the  $t_{50}$  and *in vivo* life span are essential. Conversely, SMPs are more likely to react to biostimulus, eventually affecting their stability and applications. As discussed in previous sections, cross-linking of polymers is crucial in such tenders. Thus, their suitability is usually determined by their 3D polymeric structures and biological responses. However, the degradation can be controlled by the input of desirable masses of precursors.<sup>116</sup> For example, Woodard et al. prepared the SMPs based on PCL–PLLA semi-interpenetrating networks and assessed their biodegradation behavior. The study underlines that the phase separation and a reduction in PCL's crystallinity caused the polymer to undergo surface erosion and break down within 72 h.<sup>117</sup> As a result, these materials can only be used for short-term purposes and are not appropriate for long-term applications, such as stent materials.

**6.3. Preparation Methods.** At specific stimuli, SMPs and SHPs re-establish the necessary structure and morphology. For various biological applications at once, the SMPs are advantageous, since they often support and assist self-healing. However, these desired qualities are impacted by synthesis processes, cross-linking, crystallinity, and polymer density.<sup>118</sup> Additionally, it has been noted that the spinning method had a noticeable impact on the shape memory behavior of the PU yarns, thus affecting its responses.<sup>119</sup> The preparation techniques typically govern the cross-linking, polymer masses, and densities, ultimately determining the stimulus response's outcome. Thus, the synthesis route plays a crucial role in designing SMPs. For example, Rahmatabadi et al. printed a two-layer structure of two thermoplastics, ABS and PCL, as well as TPU, an elastomer filament. The elastomeric layer was constrained by a thermoplastic layer. It became possible to stabilize the temporary shape and store the deformation stress for later recovery by a phase-changing thermoplastic layer in the opposite direction during a rubber-to-glass transition. Hence, the SME was incorporated by the 4D printing technique, which ultimately governed the response behavior upon stimulus.<sup>120</sup>

**6.4. Sterilization and Packaging.** Biomedical equipment must be packaged, sterilized, stored, and transported to the

physician for use after creation. SMP storage and packaging provide significant hurdles. As stated, the sterilization process requires a typical experience in terms of human resources and technologies. The sterilization process may be *in situ* and *ex-situ*; however, both have their respective drawbacks, as the packaging process can affect *in situ* sterilization, and the external environment may harm the *ex-situ* sterilization process. Additionally, using SMPs in the clinic necessitates cleaning and sterilization procedures that preserve physicochemical, thermomechanical, and shape recovery qualities. Ramaraju et al. tested disinfection methods using 70% ethanol and UV254 nm for clinical purposes, including ethylene oxide (ETO) gas sterilization. Although the physicochemical material qualities of the samples after 0.5 and 1 min of ethanol disinfection remained unchanged, after 15 min, they had slower recovery rates than controls.<sup>121</sup> Such incidences indicate the sterilization and packaging limitation, as preactivation may occur and affect the biomedical application of the SMPs and SHPs.

## 7. FUTURE PROSPECTIVES

SMPs and SHPs have a more extensive range of applications due to their advantages, such as high adaptability, biocompatibility, and low cost, including biomedical devices, biomedicines, scaffolds, and tissue engineering. However, as discussed above, different obstacles restrict the use of SMPs and SHPs in limited fields. The transition temperature of biobased SMPs can be adjusted for various biomedical applications. SMPs are also blended with other polymers to adapt or vary the SMEs. For instance, they can be used with biocompatible epoxy resins to adjust their thermal and mechanical needs. Epoxy resin additions aid in fine-tuning mechanical and thermal properties by including some external elements such as graphene oxide and SiO<sub>2</sub> NPs.<sup>122</sup>

Another potential application of SHPs and SMPs is their utilization as a drug delivery vehicle. Several biopolymeric materials can be blended with the SHPs to deliver stimuli-responsive drugs. Especially in cancer research, the pH at the cancer site remains slightly acidic, i.e., 5 to 6. Various polymers have been scrutinized to deliver anticancer drugs at the said pH, yet their rapid degradation is an obstacle to their long-term applicability. To solve this, a state-of-the-art blend of SHPs can be mixed with the biopolymers such as chitosan and glucuronic acid,<sup>123</sup> which in return shall provide a self-healing pH-triggered delivery of an anticancer drug.

Redox sensitivity is a brand-new, widely accepted method for creating stimuli-reactive carriers to transport pharmaceuticals. However, the redox stimulus mainly generates reactive oxygen species (ROS), which trigger antimicrobial and anticancerous activity.<sup>124</sup> Hence, amalgamating ROS production at a change in redox reaction can help design new nanomedicines, which can be used for long-term applications. For instance, a redox-responsive self-healing polymer that produces ROS might provide a long-term solution to dangerous chemotherapy to treat cancer. Further, SMPs and SHPs can also be utilized as theranostic agents. For example, these polymers can be blended with the photoluminescence carbon nanodots for conductivity-based optical sensing<sup>125</sup> and can be used for various biomedical applications such as cancer treatment, kidney stone removal, the opening of artery blockage, etc.

The expanding ability of SHPs to overcome material limitations and ensure repetitive recovery serves for improved

performance, increased service life, and a lower environmental impact. Subsequently, SMPs have great potential in tissue engineering applications, surpassing the limitations of standardized materials. These polymers have great potential in the biomedical sectors, including therapeutic to theranostic applications, which technological developments and state-of-the-art polymer design, manufacture, and characterization techniques can achieve.

## 8. CONCLUSION

In this review, the use of shape memory-assisted self-healing polymeric composites in biomedical fields such as soft robotics, drug delivery, 4D bioprinting, and tissue engineering is explored. Self-healing by using a precise mechanism of healing can recover the damage to the polymeric composite, but its efficacy in completely recovering the structure is not assured. Shape memory-assisted self-healing ensures the complete healing of the polymeric matrix after damage. It considerably aids in enhancing the mechanical properties. Researchers in tissue engineering are using this approach to construct scaffolds for minimally invasive implantation, which enhances patient compliance. Drugs released from the self-healing shape memory hydrogel can be controlled by modulating its stiffness in response to external stimuli such as light, temperature, pH, etc. Moreover, in 4D printing, intrinsically self-healing hydrogels are used as bioink that automatically reconstructs through dynamic reversible interaction after extruding through the nozzle. The printed hydrogel's self-healing properties are highly desired for fostering interlayer adhesion and enhancing the structural integrity of the deployable scaffold. In contrast, the shape memory of the scaffold enables minimally invasive delivery to fill the defect. Furthermore, the reversibility of the temporary linkage present in the shape memory polymers, along with the covalent linkage, provides the actuating force required for soft actuators. Along with easy actuation, shape memory-assisted self-healing also bestows high strength and flexibility to the soft actuators, which is necessary for their dynamic adaptation for intended applications. To control the response over precise stimuli, biodegradation, preparation routes, sterilization, and packaging are a few of the major challenges for a biomedical researcher, which can be overcome by tuning the polymeric matrix densities and cross-linkings. Further, adding a range of other bio-/copolymers can be suited for the theranostic and other biomedical applications of the SMPs and SHPs.

## AUTHOR INFORMATION

### Corresponding Author

Ashok M. Raichur — Department of Materials Engineering,  
Indian Institute of Science, Bangalore 560012, India;

orcid.org/0000-0001-5042-3122; Email: amr@iisc.ac.in

### Authors

Tejaswini Tadge — Department of Materials Engineering,  
Indian Institute of Science, Bangalore 560012, India

Sonali Garje — Department of Materials Engineering, Indian  
Institute of Science, Bangalore 560012, India

Varun Saxena — Department of Materials Engineering, Indian  
Institute of Science, Bangalore 560012, India

Complete contact information is available at:

<https://pubs.acs.org/10.1021/acsomega.3c04569>

## Author Contributions

<sup>#</sup>T.T. and S.G. made an equal contribution. Data analysis and interpretation: T.T., S.G., V.S. Writing original draft: T.T., S.G., V.S. Review and Editing: V.S. Conceptualization, draft designing, formal analysis, and supervision: A.M.R.

## Notes

The authors declare no competing financial interest.

## ACKNOWLEDGMENTS

Authors are thankful to the Department of Materials Engineering, Indian Institute of Science Bangalore, and JRD Tata Memorial Librarian, IISc Bangalore for providing access to the research publications and the facilities to structure this review article.

## REFERENCES

- (1) Greco, F.; Mattoli, V. Introduction to active smart materials for biomedical applications. *Piezoelectric Nanomaterials for Biomedical Applications* **2012**, 1–27.
- (2) Yakacki, C. M.; Gall, K. Shape-memory polymers for biomedical applications. *Shape-memory polymers* **2009**, *226*, 147–175.
- (3) Li, Y.; Chen, H.; Liu, D.; Wang, W.; Liu, Y.; Zhou, S. pH-responsive shape memory poly (ethylene glycol)–poly ( $\epsilon$ -caprolactone)-based polyurethane/cellulose nanocrystals nanocomposite. *ACS Appl. Mater. Interfaces* **2015**, *7* (23), 12988–12999.
- (4) Zhang, Y.; Liao, J.; Wang, T.; Sun, W.; Tong, Z. Polyampholyte hydrogels with pH modulated shape memory and spontaneous actuation. *Adv. Funct. Mater.* **2018**, *28* (18), No. 1707245.
- (5) Li, C.; Jiao, Y.; Lv, X.; Wu, S.; Chen, C.; Zhang, Y.; Li, J.; Hu, Y.; Wu, D.; Chu, J. J. A. m.; et al. *In situ reversible tuning from pinned to roll-down superhydrophobic states on a thermal-responsive shape memory polymer by a silver nanowire film* **2020**, *12* (11), 13464–13472.
- (6) Chatterjee, T.; Dey, P.; Nando, G. B.; Naskar, K. J. Thermo-responsive shape memory polymer blends based on alpha olefin and ethylene propylene diene rubber. *Polymer* **2015**, *78*, 180–192.
- (7) Wu, S.; Li, W.; Sun, Y.; Pang, X.; Zhang, X.; Zhuang, J.; Zhang, H.; Hu, C.; Lei, B.; Liu, Y. Facile fabrication of a CD/PVA composite polymer to access light-responsive shape-memory effects. *Journal of Materials Chemistry C* **2020**, *8* (26), 8935–8941.
- (8) Zou, Y.; Wang, P.; Fang, S.; Li, H.; Yu, Y.; Liu, Y.; Zhang, H.; Guo, J. Near-infrared light-responsive shape memory hydrogels with remodeling and excellent mechanical performance. *New J. Chem.* **2022**, *46* (15), 7223–7229.
- (9) Xiao, Y.; Zhou, S.; Wang, L.; Gong, T. Electro-active shape memory properties of poly ( $\epsilon$ -caprolactone)/functionalized multi-walled carbon nanotube nanocomposite. *ACS Appl. Mater. Interfaces* **2010**, *2* (12), 3506–3514.
- (10) Tekay, E. Preparation and characterization of electro-active shape memory PCL/SEBS-g-MA/MWCNT nanocomposites. *Polymer* **2020**, *209*, No. 122989.
- (11) Gong, T.; Li, W.; Chen, H.; Wang, L.; Shao, S.; Zhou, S. Remotely actuated shape memory effect of electrospun composite nanofibers. *Acta Biomaterialia* **2012**, *8* (3), 1248–1259.
- (12) Cai, Y.; Jiang, J.-S.; Liu, Z.-W.; Zeng, Y.; Zhang, W.-G. Magnetically-sensitive shape memory polyurethane composites cross-linked with multi-walled carbon nanotubes. *Composites Part A: Applied Science and Manufacturing* **2013**, *53*, 16–23.
- (13) Rainer, W. C.; Redding, E. M.; Hitov, J. J.; Sloan, A. W.; Stewart, W. D. *Polyethylene product and process*. Google Patents: US3144398, 1964.
- (14) Wang, S.; Urban, M. W. Self-healing polymers. *Nature Reviews Materials* **2020**, *5* (8), 562–583.
- (15) Luo, X.; Mather, P. T. Shape memory assisted self-healing coating. *ACS Macro Lett.* **2013**, *2* (2), 152–156.
- (16) Yan, K.; Xu, F.; Wang, C.; Li, Y.; Chen, Y.; Li, X.; Lu, Z.; Wang, D. J. A multifunctional metal-biopolymer coordinated double network hydrogel combined with multi-stimulus responsiveness, self-healing, shape memory and antibacterial properties. *B. S.* **2020**, *8* (11), 3193–3201.
- (17) Rousseau, I. A. J. Challenges of shape memory polymers: A review of the progress toward overcoming SMP's limitations. *P. E.; Science* **2008**, *48* (11), 2075–2089.
- (18) Behera, P. K.; Mohanty, S.; Gupta, V. K. J. Self-healing elastomers based on conjugated diolefins: a review. *P. C* **2021**, *12* (11), 1598–1621.
- (19) Behera, P. K.; Mondal, P.; Singha, N. K. J. Polyurethane with an ionic liquid crosslinker: a new class of super shape memory-like polymers. *P. c* **2018**, *9* (31), 4205–4217.
- (20) Pisani, S.; Genta, I.; Modena, T.; Dorati, R.; Bruni, G.; Benazzo, M.; Conti, B. A proof of concept to define the parameters affecting poly-l-lactide-co-poly- $\epsilon$ -caprolactone shape memory electrospun nanofibers for biomedical applications. *Drug Deliv. and Transl. Res.* **2023**, *13* (2), 593–607.
- (21) Chan, B. Q. Y.; Low, Z. W. K.; Heng, S. J. W.; Chan, S. Y.; Owh, C.; Loh, X. J. Recent advances in shape memory soft materials for biomedical applications. *J. A. a. m.; interfaces* **2016**, *8* (16), 10070–10087.
- (22) Xia, Y.; He, Y.; Zhang, F.; Liu, Y.; Leng, J. J. A review of shape memory polymers and composites: mechanisms, materials, and applications. *A. m.* **2021**, *33* (6), No. 2000713.
- (23) Behl, M.; Lendlein, A. Shape-memory polymers. *Mater. Today* **2007**, *10* (4), 20–28.
- (24) Lendlein, A.; Jiang, H.; Jünger, O.; Langer, R. Light-induced shape-memory polymers. *Nature* **2005**, *434* (7035), 879–882.
- (25) Ze, Q.; Kuang, X.; Wu, S.; Wong, J.; Montgomery, S. M.; Zhang, R.; Kovitz, J. M.; Yang, F.; Qi, H. J.; Zhao, R. J. Magnetic shape memory polymers with integrated multifunctional shape manipulation. *A. M.* **2020**, *32* (4), No. 1906657.
- (26) Xue, S.; Liu, G.; Lai, J.; An, P.; Liu, Y.; Wu, Y.; Wang, Y.; Ye, Z.; Tang, Q.; Zhou, H. J. M. M.; et al. *Boron Nitride Nanosheets Strengthened PVA/Borax Hydrogels with Highly Efficient Self-Healing and Rapid pH-Driven Shape Memory Effect* **2021**, *306* (11), No. 2100415.
- (27) Sahoo, S. D.; Ravikumar, A.; Prasad, E. PVA–Polystyrene-Based Polymer Films with Water-Induced Shape-Memory Effect. *Ind. Eng. Chem. Res.* **2022**, *61* (17), 5797–5806.
- (28) Agrawal, N.; Arora, B. J. Self-Healing Polymers and Composites: Extrinsic Routes. *M.-R. i. O. C* **2022**, *19* (4), 496–512.
- (29) Garcia, S. J. Effect of polymer architecture on the intrinsic self-healing character of polymers. *J. E. P. J.* **2014**, *53*, 118–125.
- (30) Zhu, D. Y.; Rong, M. Z.; Zhang, M. Q. Self-healing polymeric materials based on microencapsulated healing agents: From design to preparation. *J. P. i. P. S.* **2015**, *49*, 175–220.
- (31) Parameswaran, B.; Singha, N. K. Self-Healing Composites: Capsule-and Vascular-Based Extrinsic Self-Healing Systems. In *Toughened Composites*; CRC Press, 2022; pp 203–216.
- (32) Dahlke, J.; Zechel, S.; Hager, M. D.; Schubert, U. S. How to design a self-healing polymer: general concepts of dynamic covalent bonds and their application for intrinsic healable materials. *J. A. M. I.* **2018**, *5* (17), No. 1800051.
- (33) Zhang, M.; Xu, D.; Yan, X.; Chen, J.; Dong, S.; Zheng, B.; Huang, F. Self-healing supramolecular gels formed by crown ether based host–guest interactions. *J. A. C. I. E* **2012**, *51* (28), 7011–7015.
- (34) Zhang, X.; He, J. Hydrogen-bonding-supported self-healing antifogging thin films. *Sci. Rep.* **2015**, *5* (1), 9227.
- (35) Shi, L.; Ding, P.; Wang, Y.; Zhang, Y.; Ossipov, D.; Hilborn, J. Self-healing polymeric hydrogel formed by metal–ligand coordination assembly: design, fabrication, and biomedical applications. *J. M. r. c.* **2019**, *40* (7), No. 1800837.
- (36) Burattini, S.; Colquhoun, H. M.; Fox, J. D.; Friedmann, D.; Greenland, B. W.; Harris, P. J.; Hayes, W.; Mackay, M. E.; Rowan, S. J. A self-repairing, supramolecular polymer system: healability as a consequence of donor–acceptor  $\pi$ – $\pi$  stacking interactions. *J. C. c.* **2009**, *No. 44*, 6717–6719.

- (37) Ying, H.; Zhang, Y.; Cheng, J. Dynamic urea bond for the design of reversible and self-healing polymers. *J. N. c.* **2014**, *5* (1), 3218.
- (38) Pratama, P. A.; Sharifi, M.; Peterson, A. M.; Palmese, G. R. Room temperature self-healing thermoset based on the Diels–Alder reaction. *J. A. a. m.; interfaces* **2013**, *5* (23), 12425–12431.
- (39) Fu, F.; Huang, M.; Zhang, W.; Zhao, Y.; Liu, X. Thermally assisted self-healing behavior of anhydride modified polybenzoxazines based on transesterification. *Sci. Rep.* **2018**, *8* (1), 10325.
- (40) Mondal, P.; Behera, P. K.; Voit, B.; Böhme, F.; Singha, N. K. *Tailor-Made Functional Polymethacrylates with Dual Characteristics of Self-Healing and Shape-Memory Based on Dynamic Covalent Chemistry* **2020**, *305* (6), No. 2000142.
- (41) Kumar Raut, S.; Sarkar, S.; Mondal, P.; Meldrum, A.; Singha, N. K. Covalent adaptable network in an anthracenyl functionalised non-olefinic elastomer; a new class of self-healing elastomer coupled with fluorescence switching. *Chemical Engineering Journal* **2023**, *453*, No. 139641.
- (42) Banerjee, S. L.; Singha, N. K. A new class of dual responsive self-healable hydrogels based on a core crosslinked ionic block copolymer micelle prepared via RAFT polymerization and Diels–Alder “click” chemistry. *J. S. M.* **2017**, *13* (47), 9024–9035.
- (43) Abdullah, S. A.; Jumahat, A.; Abdullah, N. R.; Frommann, L. Determination of Shape Fixity and Shape Recovery Rate of Carbon Nanotube-filled Shape Memory Polymer Nanocomposites. *Procedia Engineering* **2012**, *41*, 1641–1646.
- (44) Guo, Y.; Lv, Z.; Huo, Y.; Sun, L.; Chen, S.; Liu, Z.; He, C.; Bi, X.; Fan, X.; You, Z. A biodegradable functional water-responsive shape memory polymer for biomedical applications. *J. Mater. Chem. B* **2019**, *7* (1), 123–132.
- (45) Kang, H.; Li, M.; Tang, Z.; Xue, J.; Hu, X.; Zhang, L.; Guo, B. Synthesis and characterization of biobased isosorbide-containing copolyesters as shape memory polymers for biomedical applications. *J. Mater. Chem. B* **2014**, *2* (45), 7877–7886.
- (46) Xia, Y.; He, Y.; Zhang, F.; Liu, Y.; Leng, J. A review of shape memory polymers and composites: mechanisms, materials, and applications. *Advanced materials* **2021**, *33* (6), No. 2000713.
- (47) Nguyen, T. D.; Qi, H. J.; Castro, F.; Long, K. N. A thermoviscoelastic model for amorphous shape memory polymers: incorporating structural and stress relaxation. *Journal of the Mechanics and Physics of Solids* **2008**, *56* (9), 2792–2814.
- (48) Yang, Y.; Davydovich, D.; Hornat, C. C.; Liu, X.; Urban, M. W. Leaf-inspired self-healing polymers. *Chem.* **2018**, *4* (8), 1928–1936.
- (49) Lendlein, A.; Kelch, S. Shape-memory polymers. *Angew. Chem., Int. Ed.* **2002**, *41* (12), 2034–2057.
- (50) Tobushi, H.; Okumura, K.; Hayashi, S.; Ito, N. Thermomechanical constitutive model of shape memory polymer. *Mech. Mater.* **2001**, *33* (10), 545–554.
- (51) Hornat, C. C.; Urban, M. W. Shape memory effects in self-healing polymers. *Prog. Polym. Sci.* **2020**, *102*, No. 101208.
- (52) Kim, N. E.; Park, S.; Kim, S.; Choi, J. H.; Kim, S. E.; Choe, S. H.; Kang, T. w.; Song, J. E.; Khang, G. Development of Gelatin-Based Shape-Memory Polymer Scaffolds with Fast Responsive Performance and Enhanced Mechanical Properties for Tissue Engineering Applications. *ACS Omega* **2023**, *8*, 6455.
- (53) Zhang, C.; Cai, D.; Liao, P.; Su, J.-W.; Deng, H.; Vardhanabhuti, B.; Ulery, B. D.; Chen, S.-Y.; Lin, J. 4D Printing of shape-memory polymeric scaffolds for adaptive biomedical implantation. *Acta Biomaterialia* **2021**, *122*, 101–110.
- (54) Chen, X.; Huang, Z.; Yang, Q.; Zeng, X.; Bai, R.; Wang, L. 3D biodegradable shape changing composite scaffold with programmable porous structures for bone engineering. *Biomedical Materials* **2022**, *17* (6), No. 065022.
- (55) Wu, Y.; Wang, L.; Zhao, X.; Hou, S.; Guo, B.; Ma, P. X. Self-healing supramolecular bioelastomers with shape memory property as a multifunctional platform for biomedical applications via modular assembly. *Biomaterials* **2016**, *104*, 18–31.
- (56) Qu, J.; Zhao, X.; Ma, P. X.; Guo, B. pH-responsive self-healing injectable hydrogel based on N-carboxyethyl chitosan for hepatocellular carcinoma therapy. *Acta Biomaterialia* **2017**, *58*, 168–180.
- (57) Shaabani, A.; Sedghi, R. Preparation of chitosan biguanidine/PANI-containing self-healing semi-conductive waterborne scaffolds for bone tissue engineering. *Carbohydr. Polym.* **2021**, *264*, No. 118045.
- (58) Yan, W.; Ding, Y.; Zhang, R.; Luo, X.; Sheng, P.; Xue, P.; He, J. Dual-functional polymer blends with rapid thermo-responsive shape memory and repeatable self-healing properties. *Polymer* **2022**, *239*, No. 124436.
- (59) Díez-García, I.; Eceiza, A.; Tercjak, A. Improvement of mechanical properties and self-healing efficiency by ex-situ incorporation of TiO<sub>2</sub> nanoparticles to a waterborne poly (urethane-urea). *Polymers* **2019**, *11* (7), 1209.
- (60) Caprioli, M.; Roppolo, I.; Chiappone, A.; Larush, L.; Pirri, C. F.; Magdassi, S. 3D-printed self-healing hydrogels via Digital Light Processing. *Nat. Commun.* **2021**, *12* (1), 2462.
- (61) Xue, S.; Liu, G.; Lai, J.; An, P.; Liu, Y.; Wu, Y.; Wang, Y.; Ye, Z.; Tang, Q.; Zhou, H. Boron Nitride Nanosheets Strengthened PVA/Borax Hydrogels with Highly Efficient Self-Healing and Rapid pH-Driven Shape Memory Effect. *Macromol. Mater. Eng.* **2021**, *306* (11), No. 2100415.
- (62) Khademhosseini, A.; Langer, R. A decade of progress in tissue engineering. *Nat. Protoc.* **2016**, *11* (10), 1775–1781.
- (63) Hinderer, S.; Brauchle, E.; Schenke-Layland, K. Generation and assessment of functional biomaterial scaffolds for applications in cardiovascular tissue engineering and regenerative medicine. *Adv. Healthcare Mater.* **2015**, *4* (16), 2326–2341.
- (64) Shaabani, A.; Sedghi, R.; Motasadzadeh, H.; Dinarvand, R. Self-healable conductive polyurethane with the body temperature-responsive shape memory for bone tissue engineering. *Chemical Engineering Journal* **2021**, *411*, No. 128449.
- (65) Yang, L.; Wang, Z.; Fei, G.; Xia, H. Polydopamine particles reinforced poly (vinyl alcohol) hydrogel with NIR light triggered shape memory and self-healing capability. *Macromol. Rapid Commun.* **2017**, *38* (23), No. 1700421.
- (66) Lu, L.; Tian, T.; Wu, S.; Xiang, T.; Zhou, S. A pH-induced self-healable shape memory hydrogel with metal-coordination cross-links. *Polym. Chem.* **2019**, *10* (15), 1920–1929.
- (67) Sun, S.; Chen, C.; Zhang, J.; Hu, J. Biodegradable smart materials with self-healing and shape memory function for wound healing. *RSC Adv.* **2023**, *13* (5), 3155–3163.
- (68) Kang, J.; Son, D.; Wang, G.-J. N.; Liu, Y.; Lopez, J.; Kim, Y.; Oh, J. Y.; Katsumata, T.; Mun, J.; Lee, Y.; Jin, L.; Tok, J. B.-H.; Bao, Z. Tough and water-insensitive self-healing elastomer for robust electronic skin. *Adv. Mater.* **2018**, *30* (13), No. 1706846.
- (69) Yoshida, S.; Ejima, H.; Yoshie, N. Tough elastomers with superior self-recoverability induced by bioinspired multiphase design. *Adv. Funct. Mater.* **2017**, *27* (30), No. 1701670.
- (70) Li, G.; Wang, Y.; Wang, S.; Liu, Z.; Liu, Z.; Jiang, J. A thermo- and moisture-responsive zwitterionic shape memory polymer for novel self-healable wound dressing applications. *Macromol. Mater. Eng.* **2019**, *304* (3), No. 1800603.
- (71) Wischke, C.; Neffe, A. T.; Lendlein, A. Controlled drug release from biodegradable shape-memory polymers. *Shape-Memory Polymers* **2009**, *226*, 177–205.
- (72) Basu, S.; Pacelli, S.; Paul, A. Self-healing DNA-based injectable hydrogels with reversible covalent linkages for controlled drug delivery. *Acta Biomaterialia* **2020**, *105*, 159–169.
- (73) Davidson-Rozenfeld, G.; Stricker, L.; Simke, J.; Fadeev, M.; Vázquez-González, M.; Ravoo, B. J.; Willner, I. Light-responsive arylazopyrazole-based hydrogels: their applications as shape-memory materials, self-healing matrices and controlled drug release systems. Electronic supplementary information (ESI) available: Polymer characterization, loading ratio effect on hydrogel properties, amino-AAP synthesis and characterization. See DOI: 10.1039/c9py00559e. *Polym. Chem.* **2019**, *10* (30), 4106–4115.

- (74) Liu, X.; Zhang, J.; Fadeev, M.; Li, Z.; Wulf, V.; Tian, H.; Willner, I. Chemical and photochemical DNA “gears” reversibly control stiffness, shape-memory, self-healing and controlled release properties of polyacrylamide hydrogels. *Chemical Science* **2019**, *10* (4), 1008–1016.
- (75) Wang, C.; Liu, X.; Wulf, V.; Vázquez-González, M.; Fadeev, M.; Willner, I. DNA-based hydrogels loaded with Au nanoparticles or Au nanorods: thermoresponsive plasmonic matrices for shape-memory, self-healing, controlled release, and mechanical applications. *ACS Nano* **2019**, *13* (3), 3424–3433.
- (76) Xu, Y.; Yang, H.; Zhu, H.; Jiang, L.; Yang, H. Self-healing gelatin-based shape memory hydrogels via quadruple hydrogen bonding and coordination crosslinking for controlled delivery of 5-fluorouracil. *Journal of Biomaterials Science, Polymer Edition* **2020**, *31* (6), 712–728.
- (77) Wang, C.; Fischer, A.; Ehrlich, A.; Nahmias, Y.; Willner, I. Biocatalytic reversible control of the stiffness of DNA-modified responsive hydrogels: Applications in shape-memory, self-healing and autonomous controlled release of insulin. *J. C. S.* **2020**, *11* (17), 4516–4524.
- (78) Qiao, L.; Liu, C.; Liu, C.; Zong, L.; Gu, H.; Wang, C.; Jian, X. Self-healing, pH-sensitive and shape memory hydrogels based on acylhydrazone and hydrogen bonds. *Eur. Polym. J.* **2022**, *162*, No. 110838.
- (79) Nayak, S.; Prasad, S. R.; Mandal, D.; Das, P. Hybrid DNA–Carbon Dot–Poly (vinylpyrrolidone) Hydrogel with Self-Healing and Shape Memory Properties for Simultaneous Trackable Drug Delivery and Visible-Light-Induced Antimicrobial Photodynamic Inactivation. *J. A. A. B. M.* **2020**, *3* (11), 7865–7875.
- (80) Gao, B.; Yang, Q.; Zhao, X.; Jin, G.; Ma, Y.; Xu, F. 4D bioprinting for biomedical applications. *J. T. i. b.* **2016**, *34* (9), 746–756.
- (81) Wan, Z.; Zhang, P.; Liu, Y.; Lv, L.; Zhou, Y. Four-dimensional bioprinting: Current developments and applications in bone tissue engineering. *J. A. A. B. M.* **2020**, *101*, 26–42.
- (82) Kim, S. H.; Seo, Y. B.; Yeon, Y. K.; Lee, Y. J.; Park, H. S.; Sultan, M. T.; Lee, J. M.; Lee, J. S.; Lee, O. J.; Hong, H. 4D-bioprinted silk hydrogels for tissue engineering. *Biomaterials* **2020**, *260*, No. 120281.
- (83) Costa, P. D.; Costa, D. C.; Correia, T. R.; Gaspar, V. M.; Mano, J. F. Natural origin biomaterials for 4D bioprinting tissue-like constructs. *J. A. M. T.* **2021**, *6* (10), No. 2100168.
- (84) Wu, S.-D.; Hsu, S.-h. 4D bioprintable self-healing hydrogel with shape memory and cryopreserving properties. *J. B.* **2021**, *13* (4), No. 045029.
- (85) Kuang, X.; Chen, K.; Dunn, C. K.; Wu, J.; Li, V. C.; Qi, H. J. 3D printing of highly stretchable, shape-memory, and self-healing elastomer toward novel 4D printing. *J. A. A. M.; interfaces* **2018**, *10* (8), 7381–7388.
- (86) Diba, M.; Koons, G. L.; Bedell, M. L.; Mikos, A. G. 3D printed colloidal biomaterials based on photo-reactive gelatin nanoparticles. *Biomaterials* **2021**, *274*, No. 120871.
- (87) Wang, Z.; Gu, J.; Zhang, D.; Zhang, Y.; Chen, J. Structurally Dynamic Gelatin-Based Hydrogels with Self-Healing, Shape Memory, and Cytocompatible Properties for 4D Printing. *Biomacromolecules* **2023**, *24* (1), 109–117.
- (88) Bilodeau, R. A.; Kramer, R. K. Self-healing and damage resilience for soft robotics: A review. *Front. Robot. AI* **2017**, *4*, 48.
- (89) Cianchetti, M.; Laschi, C.; Mencias, A.; Dario, P. Biomedical applications of soft robotics. *J. N. R. M.* **2018**, *3* (6), 143–153.
- (90) Schönfeld, D.; Chalissery, D.; Wenz, F.; Specht, M.; Eberl, C.; Pretsch, T. Actuating shape memory polymer for thermoresponsive soft robotic gripper and programmable materials. *J. M.* **2021**, *26* (3), 522.
- (91) Roels, E.; Terryn, S.; Iida, F.; Bosman, A. W.; Norvez, S.; Clemens, F.; Van Assche, G.; Vanderborgh, B.; Brancart, J. Processing of Self-Healing Polymers for Soft Robotics. *J. A. M.* **2022**, *34* (1), No. 2104798.
- (92) Banerjee, S. L.; Swift, T.; Hoskins, R.; Rimmer, S.; Singha, N. K. A muscle mimetic polyelectrolyte–nanoclay organic–inorganic hybrid hydrogel: its self-healing, shape-memory and actuation properties. *J. Mater. Chem. B* **2019**, *7* (9), 1475–1493.
- (93) Abdullah, T.; Okay, O. 4D Printing of Body Temperature-Responsive Hydrogels Based on Poly (acrylic acid) with Shape-Memory and Self-Healing Abilities. *ACS Applied Bio Materials* **2023**, *6*, 703.
- (94) Zhao, L.; Huang, J.; Wang, T.; Sun, W.; Tong, Z. Multiple Shape Memory, Self-Healable, and Supertough PAA-GO-Fe<sup>3+</sup>-Hydrogel. *Macromol. Mater. Eng.* **2017**, *302* (2), No. 1600359.
- (95) Xue, S.; Wu, Y.; Liu, G.; Guo, M.; Liu, Y.; Zhang, T.; Wang, Z. Hierarchically reversible crosslinking polymeric hydrogels with highly efficient self-healing, robust mechanical properties, and double-driven shape memory behavior. *Journal of Materials Chemistry A* **2021**, *9* (9), 5730–5739.
- (96) Lv, Y.; Pan, Z.; Song, C.; Chen, Y.; Qian, X. Locust bean gum/gellan gum double-network hydrogels with superior self-healing and pH-driven shape-memory properties. *Soft Matter* **2019**, *15* (30), 6171–6179.
- (97) Wu, S.; Guo, J.; Wang, Y.; Xie, H.; Zhou, S. Cryopolymerized polyampholyte gel with antidehydration, self-healing, and shape-memory properties for sustainable and tunable sensing electronics. *J. A. A. M.; Interfaces* **2022**, *14* (37), 42317–42327.
- (98) Xiao, G.; Wang, Y.; Zhang, H.; Zhu, Z.; Fu, S. Cellulose nanocrystal mediated fast self-healing and shape memory conductive hydrogel for wearable strain sensors. *Int. J. Biol. Macromol.* **2021**, *170*, 272–283.
- (99) Ling, H.; Shen, Y.; Xu, L.; Pan, H.; Shen, N.; Li, K.; Ni, K. Preparation and characterization of dual-network interpenetrating structure hydrogels with shape memory and self-healing properties. *Colloids Surf., A* **2022**, *636*, No. 128061.
- (100) Zhang, W.; Leng, X.; Gao, M.; Wei, Z.; Wang, Y.; Li, Y. Synthesis of cross-linked triple shape memory polyurethane with self-healing functionalities. *Polym. Test.* **2021**, *96*, No. 107099.
- (101) Kim, H.; Julius, A. A.; Kim, M. Obstacle avoidance for bacteria-powered microrobots. In *Microbiorobotics*; Elsevier, 2017; pp 81–105.
- (102) Yazdimamaghani, M.; Razavi, M.; Vashae, D.; Moharamzadeh, K.; Boccaccini, A. R.; Tayebi, L. Porous magnesium-based scaffolds for tissue engineering. *Materials Science and Engineering: C* **2017**, *71*, 1253–1266.
- (103) Karunakaran, R.; Ortgies, S.; Tamayol, A.; Bobaru, F.; Sealy, M. P. Additive manufacturing of magnesium alloys. *Bioactive Materials* **2020**, *5* (1), 44–54.
- (104) Song, G. L.; Atrens, A. Corrosion mechanisms of magnesium alloys. *Adv. Eng. Mater.* **1999**, *1* (1), 11–33.
- (105) Fu, W.; Yang, H.; Li, T.; Sun, J.; Guo, S.; Fang, D.; Qin, W.; Ding, X.; Gao, Y.; Sun, J. Enhancing corrosion resistance of ZK60 magnesium alloys via Ca microalloying: The impact of nanoscale precipitates. *Journal of Magnesium and Alloys* **2022**, DOI: 10.1016/j.jma.2022.06.011.
- (106) Janbozorgi, M.; Karimi Taheri, K.; Karimi Taheri, A. Microstructural evolution, mechanical properties, and corrosion resistance of a heat-treated Mg alloy for the bio-medical application. *Journal of Magnesium and Alloys* **2019**, *7* (1), 80–89.
- (107) Lin, Z.; Sun, X.; Yang, H. The Role of Antibacterial Metallic Elements in Simultaneously Improving the Corrosion Resistance and Antibacterial Activity of Magnesium Alloys. *Materials & Design* **2021**, *198*, No. 109350.
- (108) Tang, J.; Wang, J.; Xie, X.; Zhang, P.; Lai, Y.; Li, Y.; Qin, L. Surface coating reduces degradation rate of magnesium alloy developed for orthopaedic applications. *Journal of Orthopaedic Translation* **2013**, *1* (1), 41–48.
- (109) Zhao, Y.; James, M. I.; Li, W. K.; Wu, G.; Wang, C.; Zheng, Y.; Yeung, K. W.; Chu, P. K. Enhanced antimicrobial properties, cytocompatibility, and corrosion resistance of plasma-modified biodegradable magnesium alloys. *Acta biomaterialia* **2014**, *10* (1), 544–556.



(110) Zhang, J.; Wei, J.; Li, B.; Zhao, X.; Zhang, J. Long-term corrosion protection for magnesium alloy by two-layer self-healing superamphiphobic coatings based on shape memory polymers and attapulgite. *J. Colloid Interface Sci.* **2021**, *594*, 836–847.

(111) Bi, H.; Ye, G.; Sun, H.; Ren, Z.; Gu, T.; Xu, M. Mechanically robust, shape memory, self-healing and 3D printable thermoreversible cross-linked polymer composites toward conductive and biomimetic skin devices applications. *J. A. M.* **2022**, *49*, No. 102487.

(112) Lan, J.; Ni, X.; Zhao, C.; Liu, Q.; Chen, C. Multiamine-induced self-healing poly (Acrylic Acid) hydrogels with shape memory behavior. *Polym. J.* **2018**, *50* (7), 485–493.

(113) Zhou, Q.; Dong, X.; Xiong, Y.; Zhang, B.; Lu, S.; Wang, Q.; Liao, Y.; Yang, Y.; Wang, H. Multi-responsive lanthanide-based hydrogel with encryption, naked eye sensing, shape memory, self-healing, and antibacterial activity. *J. A. a. m.; interfaces* **2020**, *12* (25), 28539–28549.

(114) Du, H.; Yao, Y.; Zhou, X.; Zhao, Y. Two-way shape memory behavior of styrene-based bilayer shape memory polymer plate **2023**, *34* (1), 252–260.

(115) Lee, K.; Choi, W.; Kim, S. Y.; Lee, E.-B.; Oh, W. T.; Park, J.; Lee, C. H.; Lee, J. S.; Bae, H. W.; Jang, D.-S.; Lee, K. S.; Yi, S. W.; Kang, M.-L.; Kim, C. Y.; Sung, H.-J. Laser-Responsive Shape Memory Device to Program the Stepwise Control of Intraocular Pressure in Glaucoma. *Adv Funct Materials* **2023**, No. 2300264.

(116) Lendlein, A.; Langer, R. Biodegradable, Elastic Shape-Memory Polymers for Potential Biomedical Applications. *Science* **2002**, *296* (5573), 1673–1676.

(117) Woodard, L. N.; Page, V. M.; Kmetz, K. T.; Grunlan, M. A. PCL-PLLA Semi-IPN Shape Memory Polymers (SMPs): Degradation and Mechanical Properties. *2016* **2016**, *37* (23), 1972–1977.

(118) Fulati, A.; Uto, K.; Ebara, M. Influences of Crystallinity and Crosslinking Density on the Shape Recovery Force in Poly ( $\epsilon$ -Caprolactone)-Based Shape-Memory Polymer Blends. *J. P.* **2022**, *14* (21), 4740.

(119) Benecke, L.; Tonndorf, R.; Cherif, C.; Aibibu, D. Influence of Spinning Method on Shape Memory Effect of Thermoplastic Polyurethane Yarns **2023**, *15* (1), 239.

(120) Rahmatatabadi, D.; Aberoumand, M.; Soltanmohammadi, K.; Soleyman, E.; Ghasemi, I.; Baniassadi, M.; Abrinia, K.; Zolfagharian, A.; Bodaghi, M.; Baghani, M. A New Strategy for Achieving Shape Memory Effects in 4D Printed Two-Layer Composite Structures **2022**, *14* (24), 5446.

(121) Ramaraju, H.; McAtee, A. M.; Akman, R. E.; Verga, A. S.; Bocks, M. L.; Hollister, S. J. Sterilization effects on poly(glycerol dodecanedioate): A biodegradable shape memory elastomer for biomedical applications **2023**, *111* (4), 958–970.

(122) Sahu, M.; Raichur, A. M. Synergistic effect of nanotextured graphene oxide modified with hollow silica microparticles on mechanical and thermal properties of epoxy nanocomposites. *Composites Part B: Engineering* **2022**, *245*, No. 110175.

(123) Narayan, R.; Gadag, S.; Mudakavi, R. J.; Garg, S.; Raichur, A. M.; Nayak, Y.; Kini, S. G.; Pai, K. S. R.; Nayak, U. Y. Mesoporous silica nanoparticles capped with chitosan-glucuronic acid conjugate for pH-responsive targeted delivery of 5-fluorouracil. *Journal of Drug Delivery Science and Technology* **2021**, *63*, No. 102472.

(124) Saxena, V.; Pandey, L. M. Design and characterization of biphasic ferric hydroxyapatite-zincite nanoassembly for bone tissue engineering. *Ceram. Int.* **2021**, *47* (20), 28274–28287.

(125) Jayasekhar Babu, P.; Saranya, S.; Singh, Y. D.; Venkataswamy, M.; Raichur, A. M.; Doble, M. Photoluminescence carbon nano dots for the conductivity based optical sensing of dopamine and bioimaging applications. *Opt. Mater.* **2021**, *117*, No. 111120.